AD_____

Award Number: W81XWH-11-1-0534

TITLE: RNAi Mediated Silencing of LRRK2G2019S in Parkinson's Disease

PRINCIPAL INVESTIGATOR: Howard J. Federoff, MD, PhD

CONTRACTING ORGANIZATION: Georgetown University Medical Center
Washington DC 20057-2197

REPORT DATE: August 2013

TYPE OF REPORT: Final Option Year 1

PREPARED FOR: U.S. Army Medical Research and Materiel Command
Fort Detrick, Maryland 21702-5012

DISTRIBUTION STATEMENT: Approved for Public Release;
Distribution Unlimited

REPORT DOCUMENTATION PAGE

Form Approved
OMB No. 0704-0188

1. REPORT DATE	2. REPORT TYPE	3. DATES COVERED
August 2013	Final Option Year 1	15 July 2012-14 July 2013

4. TITLE AND SUBTITLE

RNAi Mediated Silencing of LRRK2G2019S in Parkinson's Disease

5a. CONTRACT NUMBER
W81XWH-11-1-0534

5b. GRANT NUMBER
W81XWH-11-1-0534

5c. PROGRAM ELEMENT NUMBER

6. AUTHOR(S)
Howard J. Federoff, MD, PhD
Liang Huang, PhD
Xiaomin Su, PhD

E-Mail: hjf8@georgetown.edu; lh629@georgetown.edu, xs37@georgetown.edu

5d. PROJECT NUMBER

5e. TASK NUMBER

5f. WORK UNIT NUMBER

8. PERFORMING ORGANIZATION REPORT NUMBER

7. PERFORMING ORGANIZATION NAME(S) AND ADDRESS(ES)
Georgetown University Medical Center
Washington DC 20057-2197

9. SPONSORING / MONITORING AGENCY NAME(S) AND ADDRESS(ES)
U.S. Army Medical Research and Materiel Command
Fort Detrick, Maryland 21702-5012

10. SPONSOR/MONITOR'S ACRONYM(S)

11. SPONSOR/MONITOR'S REPORT NUMBER(S)

12. DISTRIBUTION / AVAILABILITY STATEMENT
Approved for Public Release; Distribution Unlimited

13. SUPPLEMENTARY NOTES

14. ABSTRACT
This proposal will utilize RNA interference technology to diminish LRRK2 kinase activity in both cell culture and animal models of G2019S-mediated neurotoxicity to establish a novel therapy for PD. To achieve this objective we proposed the following Specific Aims: 1. Inhibition of wild-type LRRK2 and G2019S expression using small interfering RNAs (siRNA), 2. *In vitro* inhibition of wild-type LRRK2 and G2019S expression using shRNA technology and 3. *In vivo* inhibition of wild-type LRRK2 and G2019S expression using shRNA technology. During this award period we completed **Technical Objective 1:** Inhibition of wild-type LRRK2 and G2019S expression using small interfering RNAs in a cell line (MN9D) with LRRK2 or G2019S overexpression to attenuate the expression of wild-type and mutant LRRK2, cell death and neurite extension. We have completed this TO. In addition we made progress on **Technical Objective 2:** *In vitro* inhibition of wild-type LRRK2 and G2019S expression using shRNA technology. We have designed and expressed shRNAs that target LRRK2 or G2019S, cloned them into viral vector expression vectors and initiated the efficacy testing *in vitro*. Lastly, we initiated work on **Technical Objective 3:** *In vivo* inhibition of wild-type LRRK2 and G2019S expression using shRNA technology. We have constructed and expressed lentivirus with expression of WT and G2019S LRRK2 and rAAV expressing shRNAs.

15. SUBJECT TERMS
RNA interference; Parkinson's disease therapy; LRRK2

16. SECURITY CLASSIFICATION OF:			17. LIMITATION OF ABSTRACT	18. NUMBER OF PAGES	19a. NAME OF RESPONSIBLE PERSON
a. REPORT	b. ABSTRACT	c. THIS PAGE			USAMRMC
U	U	U	UU		19b. TELEPHONE NUMBER *(include area code)*

Table of Contents

	Page
Introduction	2
Body	2 – 6
Key Research Accomplishments	6
Reportable Outcomes	6-7
Conclusion	7
References	7
Appendices	7

INTRODUCTION

PD is the second most common neurodegenerative disease with a prevalence ~1.5 million people in the United States. Two forms, sporadic and familial, are recognized with the sporadic form accounting for about 90% of cases. Of the six characterized familial PD genes only one, LRRK2, is prevalent in sporadic cases [1, 2]. LRRK2 mutations account for approximately 3% of familial PD; but interestingly, certain mutations in LRRK2 are also found in non-familial PD. Overall, LRRK2 mutations account for as much as 7-10% of all PD cases worldwide [3, 4]. The most frequent mutation in LRRK2 occurs at position 2019, where a glycine has been changed to a serine (G2019S) [5]. The G2019S mutation lies within the kinase domain of LRRK2 and results in upregulated kinase activity, causing a dominant gain-of-function. Additionally, mutation of the LRRK2 kinase domain (kinase dead mutants) diminishes neurotoxicity and basal kinase levels appear to be required for the toxicity of all LRRK2 mutants [6]. As the G2019S mutation accounts for both familial and non-familial forms, efforts to develop a therapeutic that inhibits LRRK2 kinase activity warrant investigation. In this application we proposed to utilize RNA interference technology to diminish LRRK2 in both cell culture and animal models of G2019S-mediated neurotoxicity to establish a novel therapy for PD. To this end we proposed the following Specific Aims: 1. Inhibition of wild-type LRRK2 and G2019S expression using small interfering RNAs (siRNA); 2. In vitro inhibition of wild-type LRRK2 and G2019S expression using shRNA technology; 3. In vivo inhibition of wild-type LRRK2 and G2019S expression using shRNA technology.

BODY

In **YEAR 1**, we have accomplished TO1 Inhibition of wild-type LRRK2 and G2019S expression using small interfering RNAs (siRNA). Specifically, we have established MN9DG2019S and MN9DLRRK2 doxycycline-inducible cell lines; characterized the cell lines quantifying cell death and neurite extension changes with LRRK2 overexpression; identified an RNAi that attenuates LRRK2 mRNA and protein expression; identified an RNAi that attenuates G2019S-mediated neurite extension pathology; demonstrated that G2019S-shRNA attenuates G2019S expression but not wild-type LRRK2 expression; and subcloned and expressed shRNAs in lentivirus and rAAV. We proposed the following technical objective for **YEAR 1 & YEAR 2**: TO2 *In vitro* inhibition of wild-type LRRK2 and G2019S expression using shRNA technology. To achieve this goal, we first evaluate the inhibition of LRRK2 expression in previously established MN9DG2019S and MN9DLRRK2 cells using lentivirus vectors that express shRNA p4 [7] or Scr shRNA (Control) (**Figure 1**). As shown in Figure 1, shRNAp4 but not Scr shRNA expression significantly decreased LRRK2 G2019S but not wild type LRRK2 mRNA and protein levels in both undifferentiated and differentiated MN9D cells. These results demonstrated efficient and specific inhibition of LRRK2 G2019S expression by shRNAp4 *in vitro*.

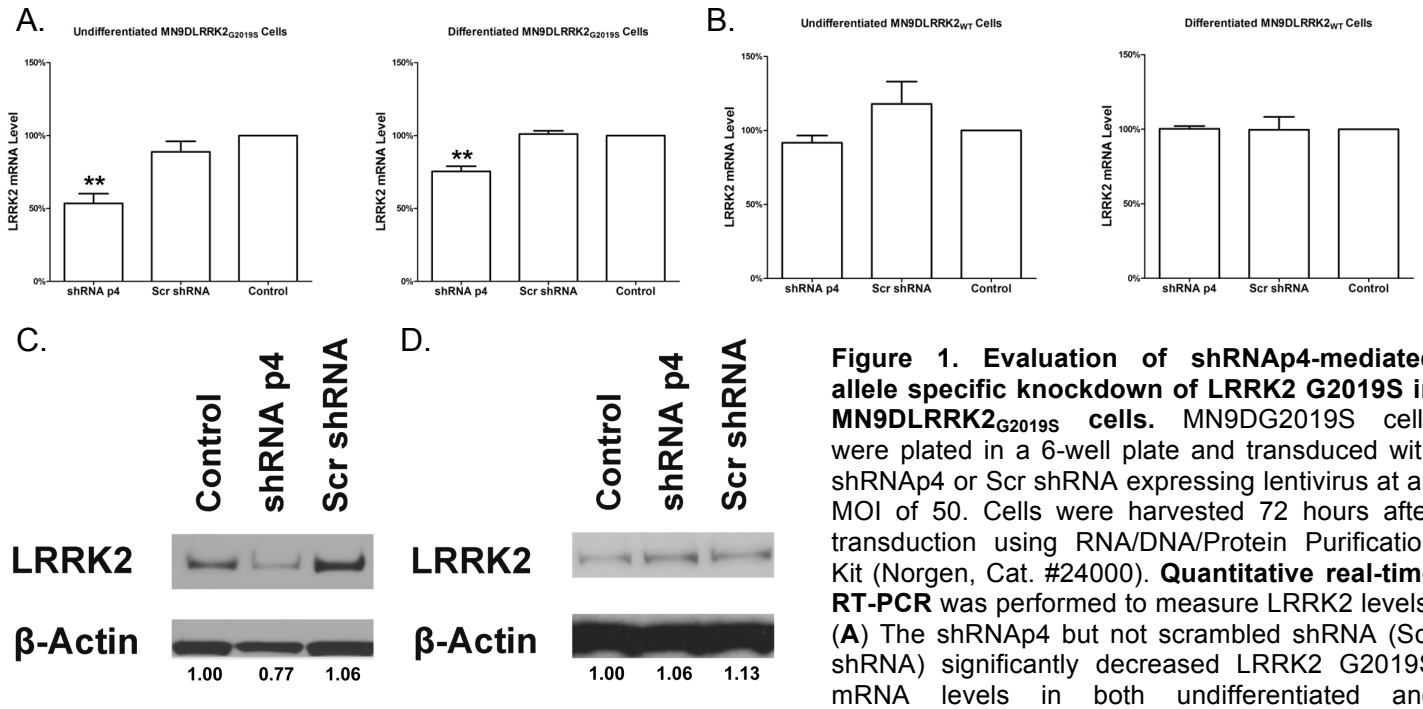

Figure 1. Evaluation of shRNAp4-mediated allele specific knockdown of LRRK2 G2019S in MN9DLRRK2$_{G2019S}$ cells. MN9DG2019S cells were plated in a 6-well plate and transduced with shRNAp4 or Scr shRNA expressing lentivirus at an MOI of 50. Cells were harvested 72 hours after transduction using RNA/DNA/Protein Purification Kit (Norgen, Cat. #24000). **Quantitative real-time RT-PCR** was performed to measure LRRK2 levels. (**A**) The shRNAp4 but not scrambled shRNA (Scr shRNA) significantly decreased LRRK2 G2019S mRNA levels in both undifferentiated and differentiated MN9DLRRK2$_{G2019S}$ cells. Only the shRNAp4 exhibited significant decrease in LRRK2 mRNA level (**p<0.01,* One-way ANOVA). Cell differentiation was induced by treating MN9DLRRK2$_{G2019S}$ cells with 2mM sodium butyrate for 6

days before transduction. Cells were then processed in the same way as undifferentiated cells. Similar to undifferentiated cells, only the shRNA p4 exhibited significant decrease in LRRK2 mRNA level (**p<0.01* One-way ANOVA). (**B**) The shRNAp4 did not inhibit wild type LRRK2 expression. No significant difference in LRRK2 mRNA level was observed in these experimental groups. Error bars indicate the standard error of the mean and represent three independent experiments. (**C**) **Western blot analysis** showing a decrease of LRRK2 G2019S protein in Lenti-shRNAp4 transduced MN9DLRRK2$_{G2019S}$ cells. Blots were probed for LRRK2 expression using a mouse monoclonal anti-human LRRK2 antibody (1:1,000 dilution; NeuroMab, Cat. #75-253). β-actin is used as a loading control. Quantitative determinations of intensities of LRRK2 signals normalized to β-actin were shown at the bottom of the western blot. (**D**) **Western blot analysis** showing no change of wild type LRRK2 protein in Lenti-shRNAp4 transduced MN9DLRRK2$_{WT}$ cells. β-actin is used as a loading control. Quantitative determinations of intensities of LRRK2 signals normalized to β-actin were shown at the bottom of the western blot.

The originally proposed outcome measurement for shRNA efficacy was decreased cell death. However, as we reported in the previous annual report, we did not observe consistently increased cell death following overexpression of either G2019S or WT LRRK2 in vitro, which precluded the use of this assay to quantify shRNA efficacy. We have hence used an alternative measure of G2019S-mediated pathophysiology by examine the neurite extension of sodium butyrate differentiate MN9D cells since LRRK2 G2019S overexpression induced a robust shortening of neurite extension. Transduction with lentiviral shRNAp4 but not the Scr shRNA reversed the neuritic shortening in DOX induced, sodium butyrate differentiated MN9DLRRK2$_{G2019S}$ cells (**Figure 2**).

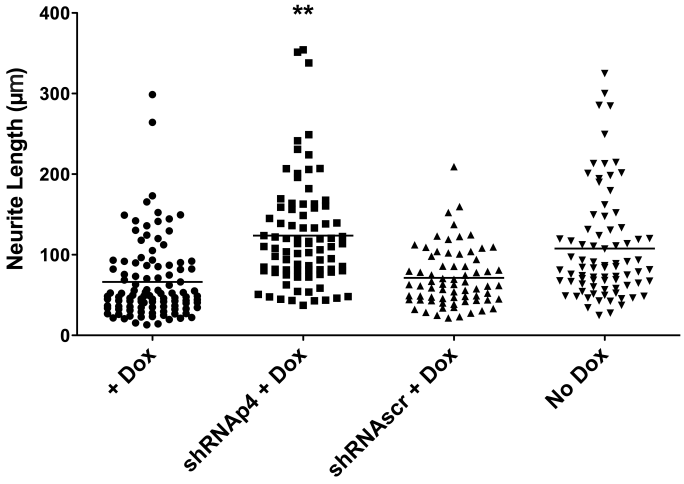

Figure 2. Neurite length shortening is reversed in MN9D$_{G2019S}$ cells following lenti-shRNAp4 transduction. MN9DLRRK2$_{G2019S}$ cells were plated on PEI coated 12-mm coverslips in a 24-well plate and differentiated with 2mM sodium butyrate for 6 days. Forty-eight hours before transduction, DOX [250ng/mL] was added to the cells to induce LRRK2 G2019S expression. Seventy-two hours after transduction, cells were fixed and immunocytochemically stained for β-tubulin. For each coverslip, pictures of 8 fields were taken and lengths of all neurites were measured using Nikon NIS Elements software. MN9DLRRK2$_{G2019S}$ without DOX induction (No Dox) was used as a control. **p<0.01 vs. control; One-way ANOVA.

Phosphorylation at Serine 910 and Serine 935 of LRRK has been implicated in LRRK2 G2019S pathology. We showed that shRNAp4 expression not only decreased total LRRK2 G2019S protein levels, but also decreased Serine 910 and Serine 935 phosphorylated LRRK2 levels (**Figure 3A**). Serine 910 and Serine 935 Phosphorylated LRRK2 wild-type proteins are not affected by shRNAp4 expression (**Figure 3B**).

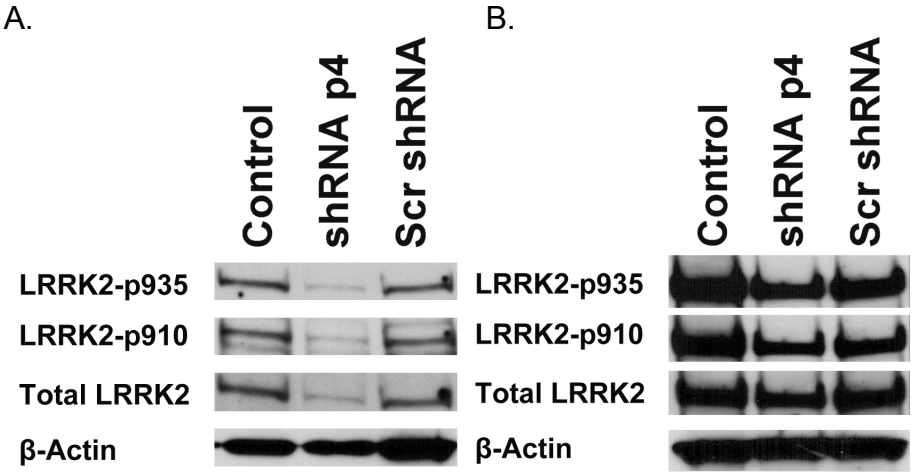

Figure 3. The shRNAp4 decreased Serine 910 and Serine 935 phosphorylated LRRK2 G2019S proteins. (**A**) Western blot showing decreases of LRRK2 phosphorylation at amino acids 910 and 935 in lenti-shRNAp4 transduced MN9DLRRK2$_{G2019S}$ cells but not in (**B**) MN9DLRRK2$_{WT}$ cells. Blots were probed with anti-LRRK2 p-S910 Rabbit monoclonal antibody (1:1000, Epticomics #5098-1) or anti-LRRK2 p-S935 Rabbit monoclonal antibody (1:1000, Epticomics #5099-1).

The above results are included in a manuscript entitled "Development of inducible leucine-rich repeat kinase 2 (LRRK2) cell lines for therapeutics development in Parkinson's disease", which has been accepted for publication in *Neurotherapeutics* in July 2013.

We next evaluated the efficiency of shRNAp4-mediated inhibition of LRRK2 G2019S expression using human PD patient fibroblasts. The LRRK2 G2019S mutant PD patient cells and normal human fibroblast Cells are originally from Coriell Institute Cell Repositories. Transient or stable expression of shRNA p4 but not Scr shRNA diminished LRRK2 G2019S protein levels in human fibroblasts in an allele specific manner (**Figure 4 and Figure 5B**).

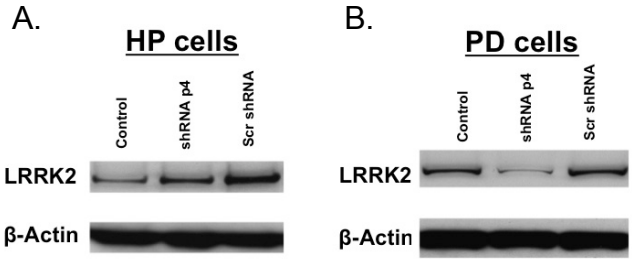

Figure 4. The shRNAp4 can specifically knockdown LRRK2 G2019S expression in human PD patient fibroblast cells. Normal human fibroblasts (HP cells) **(A)** or LRRK2 G2019S mutant PD patient fibroblasts (PD cells) **(B)** cells were transduced with Lentivirus expressing shRNAp4 or Scr shRNA. Cells were harvested 72 hours after transduction for Western blot analysis. Blots were probed with mouse monoclonal anti-human LRRK2 antibody (1:1,000 dilution; NeuroMab, Cat. #75-253).

To access the possible off-target effect of shRNA p4, we established stably transduced LRRK2 G2019S mutant PD patient cells expressing shRNA p4 or Scr shRNA (**Figure 5A**). The PD-shRNAp4 cells have a consistent lower level of LRRK2 than the PD cells and PD-Scr shRNA cells (**Figure 5B**). The gene expression profiles of the PD parental cells, PD-shRNAp4 cells, and PD-Scr shRNA cells were compared using Affymetrix microarray assays. Our data revealed no significant difference in gene expression profiles between PD-shRNAp4 and PD-Scr shRNA cells (**Figure 5C**).

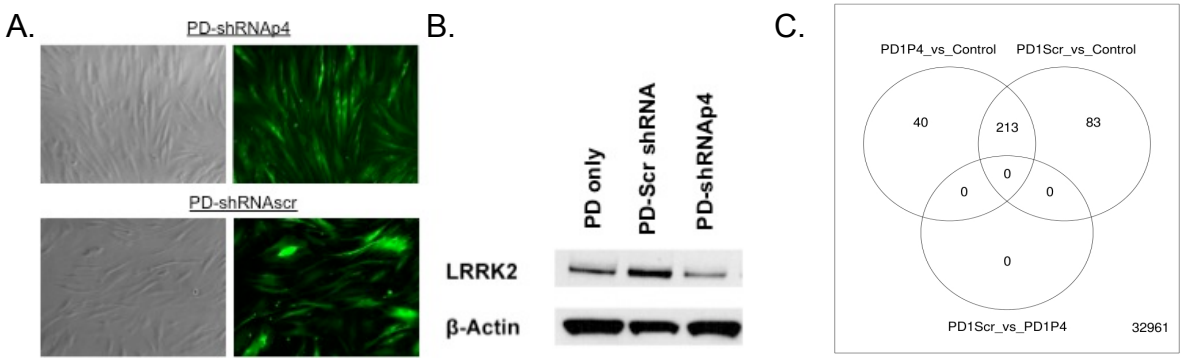

Figure 5. Accessing shRNAp4 off-targets by Affymetrix microarray analysis. (**A**) The pGreenPuro-shRNAp4 or pGreenPuro-Scr shRNA constructs that express both shRNA and GFP were delivered into PD cells by lentivirus. Stably transduced cells were selected by puromycin resistance and GFP expression. (**B**) Western blot analysis of LRRK2 expression in PD-shRNAp4, PD-Scr shRNA and the parental PD cells. (**C**) Stably transduced PD cells and the parental PD cells were harvest for total RNA. For each cell line, four replicate experiments were performed. Limma-Venn Diagram shows no significant difference between PD-shRNAp4 (PD1P4) and PD-Scr shRNA (PD1Scr) gene expressions.

We continued to work on TO3 *In vivo* inhibition of wild-type LRRK2 and G2019S expression using shRNA technology. Our objective is to utilize the most effective shRNA from TO2 and rAAV viral vector technology to express this shRNA *in vivo*. We have completed the production of rAAV-shRNAp4/GFP, shRNAscr/GFP, shRNAp4/RFP, and shRNAscr/RFP. With an improved rAAV production protocol, we are now able to produce rAAV with a viral titer as high as 10^{13} vg/mL, which should guarantee efficient delivery of our shRNA constructs. We next tested rAAV delivery of shRNA constructs *in vivo* (**Figure 6**).

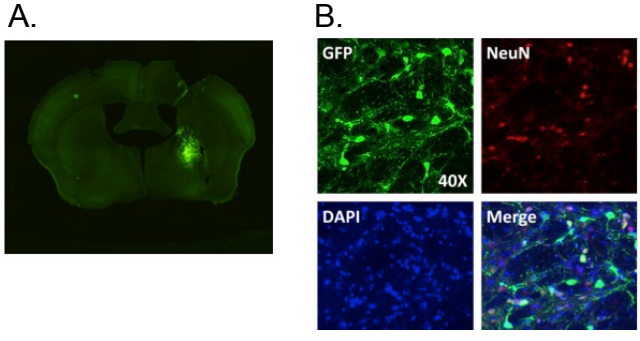

Figure 6. The rAAV-shRNAp4/GFP expression in the striatum of mouse brain. C57BL6 mouse received 5 µl of rAAV-shRNAp4/GFP stereotaxic brain injection at right striatum (posterior to bregma 0.86mm, lateral to midline 1.8mm, ventral to surface of skull 3.5mm). Seven days after injection, the animals were perfused and the brains were sectioned coronally on a

freezing sliding microtome at 40 µm through the entire brain and the sections were stored in glycol anti-freeze solution at −20°C till further processing. Immunohistochemistry was performed on free-floating sections. Every 12th brain section was chosen for NeuN and DAPI staining. (**A**) Overall view of a brain section showing the distribution of the rAAV expression. (**B**) Co-focal microscopy image detailing rAAV expression at cellular level.

As we originally proposed, we are in the process of developing rodent models that expresses human LRRK2 G2019S to test the efficiency of shRNAp4 *in vivo*. We plan to use two rodent models; the first one is a Lentiviral-mediated human LRRK2 expression on a rat LRRK2 knockout background, the second is a BAC human LRRK2 transgenic rat model also on a LRRK2 knockout background. In the first model, we decided to co-deliver human LRRK2 G2019S/GFP expressing lentivirus construct and shRNA/RFP expressing rAAV construct into LRRK2 knockout rats. To achieve this goal, we constructed C-terminal 3XFLAG tagged N-terminal truncated LRRK2 G2019S (dNLRRK2 G2019S, amino acids 1328 – 2527) lentivirus constructs to improve LRRK2 G2019S expression. This truncated protein retained the C-terminal ROC, COR, Kinase, and WD40 domains of LRRK2 [8]. Since there is no reliable LRRK2 antibody currently for immunohistochemistry (IHC), the 3XFLAG tag allows us to directly detect LRRK2 expressed *in vivo* via IHC. To achieve optimal expression of dNLRRK2 G2019S in neuronal cells *in vivo*, we replaced the original cytomegalovirus (CMV) promoter on the lentiviral vector with human phosphoglycerate kinase (hPGK) promoter or with human neuron-specific enolase (hNSE) promoter, which expresses more efficiently in neurons [9, 10]. We have tested the lentivirus vectors for dNLRRK2 G2019S expression in human 293T cells and observed robust dNLRRK2 G2019S levels in hPGK-dNLRRK2 vector transfected cells with both anti-FLAG antibody and anti-LRRK2 antibody (**Figure 7**). The hNSE-dNLRRK2 vector did not express in human 293T cells owing to the use of the neuronal specific NSE promoter. Lentiviruses carrying these vectors have been produced. We are currently in the process of examining dNLRRK2 expression in mouse and rat models.

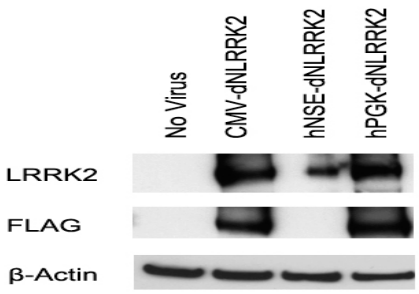

Figure 7. Evaluation of dNLRRK2 G2019S expression vectors with different promoters in human 293T cells. Human 293T cells are seeded in 12-well plates at $2.5X10^5$ cells/well. Cells were transfected with plasmids pCDH-CMV-dNLRRK2G2019S, pCDH-hNSE-dNLRRK2G2019S and pCDH-hPGK-dNLRRK2GS. Forty-eight hours after transfection, Cells were harvested with RIPA buffer and ran on a 4-12% PAGE gel for Western blot analysis. Blots were probed with anti-FLAG (1:1000, Sigma), anti-LRRK2 (1:1000, NeuroMab), and anti-β-Actin (1:2000, Abcam) antibodies.

As a proof of concept, we tested the co-transduction of rAAV and lentivirus in human HT1080 cells. As shown in **Figure 8A** (bottom right panel), we were able to locate cells that expressing both shRNAp4 and dNLRRK2 G2019S with the RFP and GFP markers located on the vectors. Co-transduction of rAAV-shRNAp4 with lenti-dNLRRK2 was able to reduce dNLRRK2 G2019S protein levels (**Figure 8B,** lentivirus:rAAV ratio at 1:20).

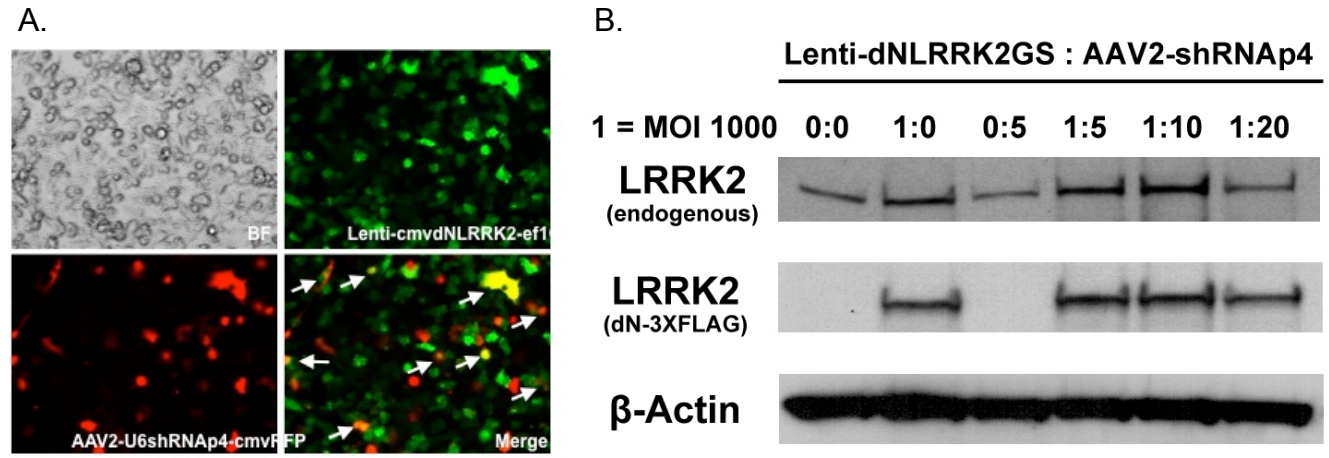

Figure 8. Co-transduction of Lenti-dNLRRK2 G2019S and AAV2-shRNAp4. HT1080 cells were plated in 6-well plates and co-transduced with Lenti-dNLRRK2 G2019S and rAAV2-shRNAp4. (**A**) Both lentivirus and AAV were expressed in HT1080 cells. Arrow heads indicate cells with both dNLRRK2 and shRNAp4 expression. (**B**) Western blot analysis for LRRK2 levels in lentivirus and AAV co-transduction HT1080 cells. A reduction of LRRK2 protein levels were observed in cells co-transduced with lentivirus:rAAV ratio at 1:20.

We recently acquired hBACLRRK2G2019S rats (hemizygous; background: Sprague Dawley) from the Oxford Parkinson's Disease Centre (OPDC). hBAC trangenic rats carry the G2019S mutant form of the LRRK2 genomic locus tagged with a fluorescent marker. The lines show robust expression of LRRK2 with a correct spatial pattern identified by direct fluorescence imaging and immunohistochemistry (**Figure 9**). We will use these animals as an additional model to investigate the efficiency of shRNAp4 *in vivo*

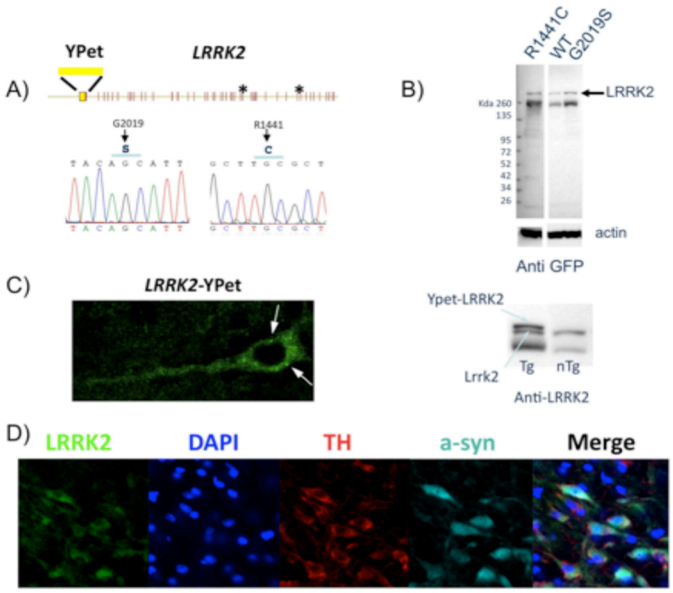

Figure 9. Construction and characterization of human BAC transgenic rats carrying the LRRK2 G2019s allele (obtained from OPDC). Characterisation of novel BAC transgenic rat lines expressing wild-type or mutant forms of LRRK2. **(A)** A BAC clone carrying the complete genomic locus of LRRK2 was modified to incorporate a 5' YPet fluorescent tag to express a YPet-LRRK2 fusion protein. The BACs express either the wild-type protein, or were engineered to express the G2019S or R1441C disease-associated mutation. **(B**) Transgenic rat lines express the LRRK2 transgene robustly as detected by either anti-GFP or anti-LRRK2 antibodies on western blot. **(C)** LRRK2-YPet expression is visible in transgenic rats by direct fluoresence imaging in cortical neurons. **(D)** Dopaminergic neurons in the substantia nigra of transgenic rats express LRRK2, TH and alpha-synuclein by immunohistochemistry.

In conclusion, we have published our data from TO1 and are currently preparing a manuscript that includes the data from TO2. **We have met the objectives for YEAR 2**. Furthermore, we are in standing to complete our goals for YEAR 3.

KEY RESEARCH ACCOMPLISHMENTS

- Demonstrated efficient and specific inhibition of LRRK2 G2019S expression by shRNA p4 in MN9D cells and human PD patient fibroblasts.
- Demonstrated that Inhibition of LRRK2 G2019S expression by shRNA p4 rescued the neurite extension shortening in Dox-induced MN9D G2019S cells.
- Showed that shRNA p4 also reduced the levels of LRRK2 Serine 910 and Serine 935 phosphorylation.
- Evaluated the possible off-target effects of shRNA p4 using Affymetrix microarray assays and showed no obvious off-targets.
- Constructed lentiviral truncate LRRK2 G2019S vectors with neuron specific promoters.
- Examined the efficiency of LRRK2 inhibition *in vitro* with co-transduced rAAV-shRNAp4 and Lenti-dNLRRKG2019S.
- Produced high quality rAAV-shRNA vectors and truncate LRRK2 G2019S lentivirus for *in vivo* study.

REPORTABLE OUTCOMES

1. Abstracts

Huang L, Su X, Wang J, Maguire-Zeiss K, and Federoff HJ. (2013), RNA Interference-Based Gene Therapy for Parkinson's Disease Using shRNA That Specifically Targeting the LRRK2 G2019S Allele. Mol. Ther. 21:S176. 16th Annual Meeting of the American Society of Gene & Cell Therapy, May 15-18, 2013, Salt Lake City, Utah.

2. Publications

Huang L, Shimoji M, Wang J, Shah S, Kamila S, Biehl ER, Lim S, Chang A, Maguire-Zeiss KA, Su X, and Federoff HJ, (Accepted, *Neurotherapeutics*), Development of Inducible Leucine-Rich Repeat Kinase 2 (LRRK2) Cell Lines for Therapeutics Development in Parkinson's Disease.

3. Manuscript under preparation
Huang L, Su X, Wang J, Maguire-Zeiss K, and Federoff HJ. “Allelle specific targeting of LRRK2 G2019S with shRNA-induced RNA interference as a potential therapeutics for Parkinson’s disease”.

4. Development of cell lines
Stably transduced LRRK2 G2019S PD patient fibroblasts that express shRNA p4 or Scr shRNA.

CONCLUSION
In conclusion, we have made substantial progress on this project. We have published our data generated in Year 1 in the journal *Neurotherapeutics*. We met the technical objectives for TO2 as we originally outlined for **Year 2** of this project. We have shown, in concept, that our system is valid to evaluate the shRNAp4 in animal models. We have made important progress to establish a LRRK2 G2019S rodent model for this purpose. **“so what section”**: The work presented here demonstrated that the shRNAp4 can attenuate LRRK2 G2019S in mouse and, importantly, human PD patient cells. In addition, our preliminary work showed robust expression of the rAAV-shRNAp4 vectors *in vivo*. Work in Year 3 will test how effectively rAAV-delivered shRNAs attenuate LRRK2 G2019S in animal models.

REFERENCES

1. Cookson, M.R., et al., *The roles of kinases in familial Parkinson's disease.* The Journal of neuroscience : the official journal of the Society for Neuroscience, 2007. **27**(44): p. 11865-8.
2. Tan, E.K. and L.M. Skipper, *Pathogenic mutations in Parkinson disease.* Human mutation, 2007. **28**(7): p. 641-53.
3. Farrer, M.J., *Genetics of Parkinson disease: paradigm shifts and future prospects.* Nature reviews. Genetics, 2006. **7**(4): p. 306-18.
4. Funayama, M., et al., *A new locus for Parkinson's disease (PARK8) maps to chromosome 12p11.2-q13.1.* Annals of neurology, 2002. **51**(3): p. 296-301.
5. Hernandez, D., et al., *The dardarin G 2019 S mutation is a common cause of Parkinson's disease but not other neurodegenerative diseases.* Neuroscience letters, 2005. **389**(3): p. 137-9.
6. West, A.B., et al., *Parkinson's disease-associated mutations in LRRK2 link enhanced GTP-binding and kinase activities to neuronal toxicity.* Human molecular genetics, 2007. **16**(2): p. 223-32.
7. Sibley, C.R. and M.J. Wood, *Identification of allele-specific RNAi effectors targeting genetic forms of Parkinson's disease.* PloS one, 2011. **6**(10): p. e26194.
8. Greggio, E., et al., *The Parkinson disease-associated leucine-rich repeat kinase 2 (LRRK2) is a dimer that undergoes intramolecular autophosphorylation.* The Journal of biological chemistry, 2008. **283**(24): p. 16906-14.
9. Li, M., et al., *Optimal promoter usage for lentiviral vector-mediated transduction of cultured central nervous system cells.* Journal of neuroscience methods, 2010. **189**(1): p. 56-64.
10. Xu, R., et al., *Quantitative comparison of expression with adeno-associated virus (AAV-2) brain-specific gene cassettes.* Gene therapy, 2001. **8**(17): p. 1323-32.

APPENDICES: Accepted manuscript

Huang L, Shimoji M, Wang J, Shah S, Kamila S, Biehl ER, Lim S, Chang A, Maguire-Zeiss KA, Su X, and Federoff HJ, (Accepted, *Neurotherapeutics*), Development of Inducible Leucine-Rich Repeat Kinase 2 (LRRK2) Cell Lines for Therapeutics Development in Parkinson’s Disease

SUPPORTING DATA: All supporting data are included in the text.

JrnlID 13311_ArtID 208_Proof# 1 - 02/08/2013

Neurotherapeutics
DOI 10.1007/s13311-013-0208-3

ORIGINAL ARTICLE

Development of Inducible Leucine-rich Repeat Kinase 2 (LRRK2) Cell Lines for Therapeutics Development in Parkinson's Disease

Liang Huang · Mika Shimoji · Juan Wang · Salim Shah · Sukanta Kamila · Edward R. Biehl · Seung Lim · Allison Chang · Kathleen A. Maguire-Zeiss · Xiaomin Su · Howard J. Federoff

Abstract The pathogenic mechanism(s) contributing to loss of dopamine neurons in Parkinson's disease (PD) remain obscure. *Leucine-rich repeat kinase 2* (*LRRK2*) mutations are linked, as a causative gene, to PD. *LRRK2* mutations are estimated to account for 10 % of familial and between 1 % and 3 % of sporadic PD. *LRRK2* proximate single nucleotide polymorphisms have also been significantly associated with idiopathic/sporadic PD by genome-wide association studies. LRRK2 is a multidomain-containing protein and belongs to the protein kinase super-family. We constructed two inducible dopaminergic cell lines expressing either human-LRRK2-wild-type or human-LRRK2-mutant (G2019S). Phenotypes of these LRRK2 cell lines were examined with respect to cell viability, morphology, and protein function with or without induction of *LRRK2* gene expression. The overexpression of *G2019S* gene promoted 1) low cellular metabolic activity without affecting cell viability, 2) blunted neurite extension, and 3) increased phosphorylation at S910 and S935. Our observations are consistent with reported general phenotypes in LRRK2 cell lines by other investigators. We used these cell lines to interrogate the biological function of LRRK2, to evaluate their potential as a drug-screening tool, and to investigate screening for small hairpin RNA-mediated *LRRK2 G2019S* gene knockdown as a potential therapeutic strategy. A proposed LRRK2 kinase inhibitor (i.e., IN-1) decreased LRRK2 S910 and S935 phosphorylation in our MN9DLRRK2 cell lines in a dose-dependent manner. Lentivirus-mediated transfer of LRRK2 G2019S allele-specific small hairpin RNA reversed the blunting of neurite extension caused by *LRRK2 G2019S* overexpression. Taken together, these inducible LRRK2 cell lines are suitable reagents for LRRK2 functional studies, and the screening of potential LRRK2 therapeutics.

Keywords Parkinson's disease (PD) · Leucine-rich repeat kinase 2 (LRRK2) · Dopaminergic cell lines · RNAi · Kinase assay · Cell viability

Introduction

The pathogenic mechanisms that cause the loss of dopamine neurons in Parkinson's disease (PD) remain obscure. *Leucine-rich repeat kinase 2* (*LRRK2*)/*Dardarin* mutations are linked, as a causative gene, to PD [1–4]. *LRRK2* mutations are estimated to account for 10 % of familial and between 1 % and 3 % of sporadic PD [5–10]. *LRRK2* proximate single nucleotide polymorphisms have also been significantly associated with idiopathic/sporadic PD by genome-wide association studies [3, 4, 11]. LRRK2 is a multi-domain containing protein and belongs to the protein kinase super-family [12, 13]. The 6 domains include: ankyrin repeats, leucine-rich repeats, a guanosine triphosphate-binding Ras of complex protein (ROC), a carboxy-terminal of ROC, a kinase domain, and a WD40 domain [14]. There are several variant forms of

Liang Huang and Mika Shimoji Joint first authors.

Electronic supplementary material The online version of this article (doi:10.1007/s13311-013-0208-3) contains supplementary material, which is available to authorized users.

L. Huang · M. Shimoji · J. Wang · S. Lim · A. Chang · K. A. Maguire-Zeiss · X. Su · H. J. Federoff (✉)
Department of Neuroscience, Georgetown University Medical Center, Washington, DC, USA
e-mail: hjf8@georgetown.edu

S. Shah · H. J. Federoff
Department of Neurology, Georgetown University Medical Center, Washington, DC, USA

S. Kamila · E. R. Biehl
Department of Chemistry, Southern Methodist University, Dallas, TX, USA

LRRK2 harboring mutations in different domains [1, 3], among which, the R1441C/G/H, Y1669C, I2020T, and G2019S mutations are known to be associated with PD [15]. These mutations are located within the ROC–carboxy-terminal of ROC-kinase domain of the LRRK2 protein, affecting the guanosine triphosphatase or the kinase activity; however, it is unclear how these changes influence the normal functions of wild-type (WT) LRRK2 [16]. However, the most frequent mutation is a single nucleotide mutation causing an amino acid substitution of glycine to serine (G2019S) [8, 11, 17]. This G2019S mutation leads to increased LRRK2 kinase activity [18–21]. Importantly, an inactivating mutation of the LRRK2 kinase domain, in concert with the G2019S mutation, has been shown to decrease neurotoxicity [13], thus implicating increased kinase activity as one of the mechanisms of LRRK2-associated PD pathogenesis.

Although the exact biological function(s) of LRRK2 and its role in biochemical pathways are under investigation, several potential substrates have been identified, including LRRK2, Akt1, ezrin/radxin/moesin (ERM) proteins, β-tubulin, eukaryotic initiation factor 4E-binding protein 1, and mitogen-activated kinase 3, 4, 6, and 7 [13, 22–34]. The functional implications of the majority of these potential substrates with respect to LRRK2 patho- and physiological actions remain uncertain. However, the work of Sheng et al. [34] has directly implicated LRRK2 Ser1292 in pathogenic effects in cultured cells.

As the LRRK2 G2019S mutation is causal and contributory to familial and sporadic/idiopathic PD respectively, together accounting for ~2 % of all PD in the North American and UK population [7, 8] and 20–40 % in certain populations [35–37], the development of models that may be predictive in the prosecution of new therapeutics is meritorious. Advancing the development of both small molecules and biologics for PD requires cellular models in which the varying and stable levels of a putative pathogenic gene product can be studied. Ideally, these studies should be undertaken in a dopaminergic background. In parallel, the examination of the WT form of the gene product in an identical context is required to ascribe the distinct pathogenic effects owing to the mutant form. Finally, the cellular models should prove useful for the demonstration that candidate therapeutics protect or reverse the pathogenic action due to putative mutant gene product.

In an effort to develop candidate therapeutics targeting LRRK G2019S we constructed two inducible dopaminergic MN9D cell lines expressing either human LRRK2-WT or human LRRK2-mutant (G2019S), each co-expressing green fluorescent protein (GFP). These LRRK2 cell lines were examined for cell viability, morphology, and LRRK2 functions with or without induction of gene expression [38]. In addition, we used these cell lines to investigate a previously described LRRK2 kinase inhibitor, IN-1 [38] and small hairpin RNA (shRNA)-mediated *LRRK2 G2019S* gene silencing. Our data, reported herein, indicate that these inducible LRRK2 cell lines are suitable for the study of LRRK2 function and for screening potential LRRK2 targeted therapeutics.

Materials and Methods

Reagents and Chemicals

Lipofectamine 2000, real-time polymerase chain reaction (PCR) universal human LRRK2 probe and Alexa-594 conjugated goat anti-rabbit IgG antibody (Ab) were from Life Technologies (Grand Island, NY, USA). Sodium bicarbonate, hygromycin, Dulbecco's Modified Eagle Medium, doxycycline (DOX), sodium butyrate, 4',6-diamidino-2-phenylindole, and trypan blue solutions were from Sigma-Aldrich (St. Louis, MO, USA). The MTS cell viability CellTiter 96 AQueous assay kit was from Promega (Madison, WI, USA). Rabbit monoclonal antihuman LRRK2 Ab, rabbit monoclonal antihuman phospho-LRRK2 S910 Ab, and rabbit monoclonal antihuman phospho-LRRK2 S935 Ab were from Epitomics (Burlingame, CA, USA). Rabbit polyclonal antibeta tubulin III Ab was from Covance (Chantilly, VA, USA). Horseradish peroxidase (HRP)-conjugated goat anti-rabbit IgG and HRP-conjugated goat anti-mouse IgG secondary Abs were from Jackson ImmunoResearch (West Grove, PA, USA). Mouse monoclonal anti-glyceraldehyde 3-phosphate dehydrogenase (GAPDH) Ab was from Millipore (Billerica, MA, USA). Rabbit monoclonal pan-Akt (C67E7), rabbit polyclonal phosphor-Akt (Ser473), and rabbit polyclonal ERM, rabbit monoclonal phospho-Ezrin(Thr567)/Radixin(Thr564)/Moesin (Thr558) (41A3) Abs were from Cell Signaling Technology (Danvers, MA, USA).

Chemical Synthesis

IN-1 was synthesized as described by Deng et al. [38].

DNA Plasmids

The full-length human *LRRK2 WT* or *G2019S* genes (7.6 kb) were subcloned in the vector plasmid with IRESeGFP, pBig2iFLAGSocs6IRES2eGFP plasmid, as described previously [39–41].

Stable Cell Lines

A mouse midbrain cell line, MN9D [42], was used for the LRRK2 stable cell line construction. MN9D cells were cultured in Dulbecco's Modified Eagle Medium supplemented with 10 % fetal bovine serum, and 3.7 g/L sodium bicarbonate at 37 °C, 5 % carbon dioxide. MN9D cells were transfected with plasmid constructs that overexpress full-length human LRRK2 WT or mutant (G2019S) and GFP under the control of a tetracycline-inducible promoter. Low passage number

MN9D cells (< 6 passage) were used for Lipofectamine 2000-mediated transfection of the LRRK2 WT or G2019S DNA according to the manufacturer's specification. Transfected cells were selected with hygromycin (500 μg/mL). These constructs also express GFP (eGFP) using an internal ribosome entry sequence (IRES). LRRK2 WT, G2019S, and eGFP expression was induced with addition of DOX (2 μg/mL). Cell colonies with eGFP expression were selected, expanded, sorted (fluorescence-activated cell sorting), and confirmed for *LRRK2 WT* or *G2019S* expression.

Western Blotting

Total protein from MN9DLRRK2$_{WT}$ and MN9DLRRK2$_{G2019S}$ cells was extracted in RIPA buffer (50 mM Tris–hydrochloric acid, pH 7.4; 1 % NP-40; 0.25 % sodium deoxycholate; 150 mM sodium chloride) containing protease inhibitors (1 mM ethylenediaminetetraacetic acid; 1 mM phenylmethylsulphonyl fluoride) or using a RNA/DNA/Protein Purification Kit (Norgen, Thorold, ON, Canada). Equal amounts of total protein (20 μg) from each sample were subjected to denaturing polyacrylamide gel electrophoresis [4–20 % Bis-Tris gradient gel (BioRad, Hercules, CA, USA) or NuPAGE Novex 3–8 % Tris-Acetate Gel (Life Technologies)]. LRRK2 protein expression levels were detected using a rabbit polyclonal anti-human LRRK2 antibody (1:5000 dilution; Epitomics/MJFF#2 [c41-2]) followed by incubation with HRP-conjugated goat anti-rabbit IgG secondary antibody (1:2000) and chemiluminescent detection (Perkin Elmer, Waltham, MA, USA). Other Abs used were GAPDH (1:20,000), rabbit polyclonal anti-human phospho-LRRK2 S910 and S935 antibodies (1:5000), rabbit monoclonal pan-Akt (C67E7) (1:1000), rabbit polyclonal anti-phospho-Akt (Ser473)(1:1000), rabbit polyclonal ERM Ab (1:1000), rabbit monoclonal anti-phospho-Ezrin(Thr567)/Radixin(Thr564)/Moesin(Thr558) (41A3) Ab (1:1000), and rabbit anti-4E-binding protein 1 Ab (1:1000).

Immunocytochemistry and Neurite Extension Assay

MN9DLRRK2$_{G2019S}$ or MN9DLRRK2$_{WT}$ 5×10^4 cells/well were plated on polyethylenemine-coated coverslips and differentiated for 6 days with 2 mM sodium butyrate. On day 6, DOX was added to induce GFP and *LRRK2 WT* or *G2019S* expression. Forty-eight hours after the addition of DOX, cells were fixed in a 4 % paraformaldehyde, 4 % sucrose solution, permeabilized in 0.1 % Triton-X-100/PBS, and blocked in 10 % normal goat serum. Cells were probed with LRRK2 Ab (1:50) or rabbit polyclonal antibeta-tubulin III Ab (1:2000) followed by Alexa-594-conjugated goat anti-rabbit IgG Ab (1:200) and 4',6-diamidino-2-phenylindole (300 nM) staining. The fluorescent labeled images were captured and analyzed with AxioVision software equipped AxioPlan2 Zeiss fluorescent microscope (Carl-Zeiss, Thornwood, NY, USA). For neurite measurements, MN9DLRRK2$_{G2019S}$ cells were plated on polyethylenemine-coated 12-mm coverslips in a 24-well plate and differentiated with 2 mM n-butyrate for 6 days. DOX (250 ng/mL) was added to induce *LRRK2 G2019S* expression for 48 h. Cells were treated with IN-1 or transduced with lenti-shRNA and subjected to immunocytochemical staining as described above. Pictures of 8 fields were taken for each sample and lengths of all beta-tubulin II-positive neurites were measured with Nikon NIS Elements software. About 40–100 neurites was measured for each condition.

RNA Interference With Lenti-shRNA

The shRNA p4 was designed according to the published LRRK2 G2019S allele-specific p4 sequence [43]. The shRNA p4 sequence 5'-GAGATTGCTGACTGCAGTACCTGACC CATGCTGTAGTCAGCAATCTCTT-3' and the scrambled shRNA (shRNA) sequence 5'-GGAATACGTACGGCTTAGT CCTGACCCAACT AAGCCGTACGTATTCCTT-3' were, respectively, cloned into the pENTR6/U6 vector (Life Technologies) and then subcloned into the pLenti6-/BLOCK-iT-DEST vector (Life Technologies) via Gateway cloning. The resulting plasmids were sequenced to confirmed accuracy. Lentivirus was packaged in 293 T cells by cotransfecting the cells with the above pLenti6-shRNA vectors and the ViraPower Packaging Mix (Life Technologies) according to the manufacturer's specifications. MN9DLRRK2$_{G2019S}$ and MN9DLRRK2$_{WT}$ cells were plated in a 6-well plate and transduced with shRNAp4 or scrambled shRNA-expressing lentivirus at a multiplicity of infection of 50. MN9DLRRK2$_{WT}$ cells were induced with 250 ng/mL DOX before transduction owing to a very low level of LRRK2 WT expression. Cells were harvested 72 h after transduction using a RNA/DNA/Protein Purification Kit (Norgen Biotek). Quantitative real-time reverse transcription-PCR was performed to measure LRRK2 mRNA levels with universal human LRRK2 probe (Life Technologies) and Applied Biosystems 7900HT Fast Real-Time PCR System. For each sample, 1 μg of total RNA was used for complementary DNA synthesis. All data were normalized to mouse GAPDH expression as an internal control. Expression of shRNA was inferred from positive expression of the *blasticidin* gene within the same construct. The LRRK2 protein expression levels were examined by western blot assays as described above.

Results

Human LRRK2 Protein Expression in MN9DLRRK2 Stable Cell Lines with Doxycycline Induction

Full-length complementary DNA of LRRK2WT or LRRK2G2019S was amplified by high-fidelity PCR and

cloned into the pBig2iFLAGSocs6IRES2eGFP, which is a tetracycline-responsive autoregulated bi-directional expression vector with an IRESeGFP cassette [39, 40]. Stably transfected human LRRK2 inducible cell lines were examined first for GFP expression and followed by fluorescence-activated cell sorting for GFP expression. Selected GFP-positive cells were expanded and confirmed for LRRK2 gene and protein expression. Undifferentiated MN9DLRRK2$_{WT}$ cells were induced with increasing concentrations of DOX (ranged from 0 to 4000 ng/mL) for 48 h. The transcription and translation of LRRK2 was turned on in response to DOX in a precise and dose-dependent manner (Fig. 1). The expression of LRRK2 mRNA in sodium butyrate-differentiated MN9DLRRK2$_{WT}$ cells followed a similar induction profile as the undifferentiated cells (Fig. 1A, top right). The expression level of LRRK2 mRNA in both undifferentiated (Fig. 1A, top left) and differentiated MN9DLRRK2$_{WT}$ cells (Fig. 1A, top right) increased approximately 10-fold in response to

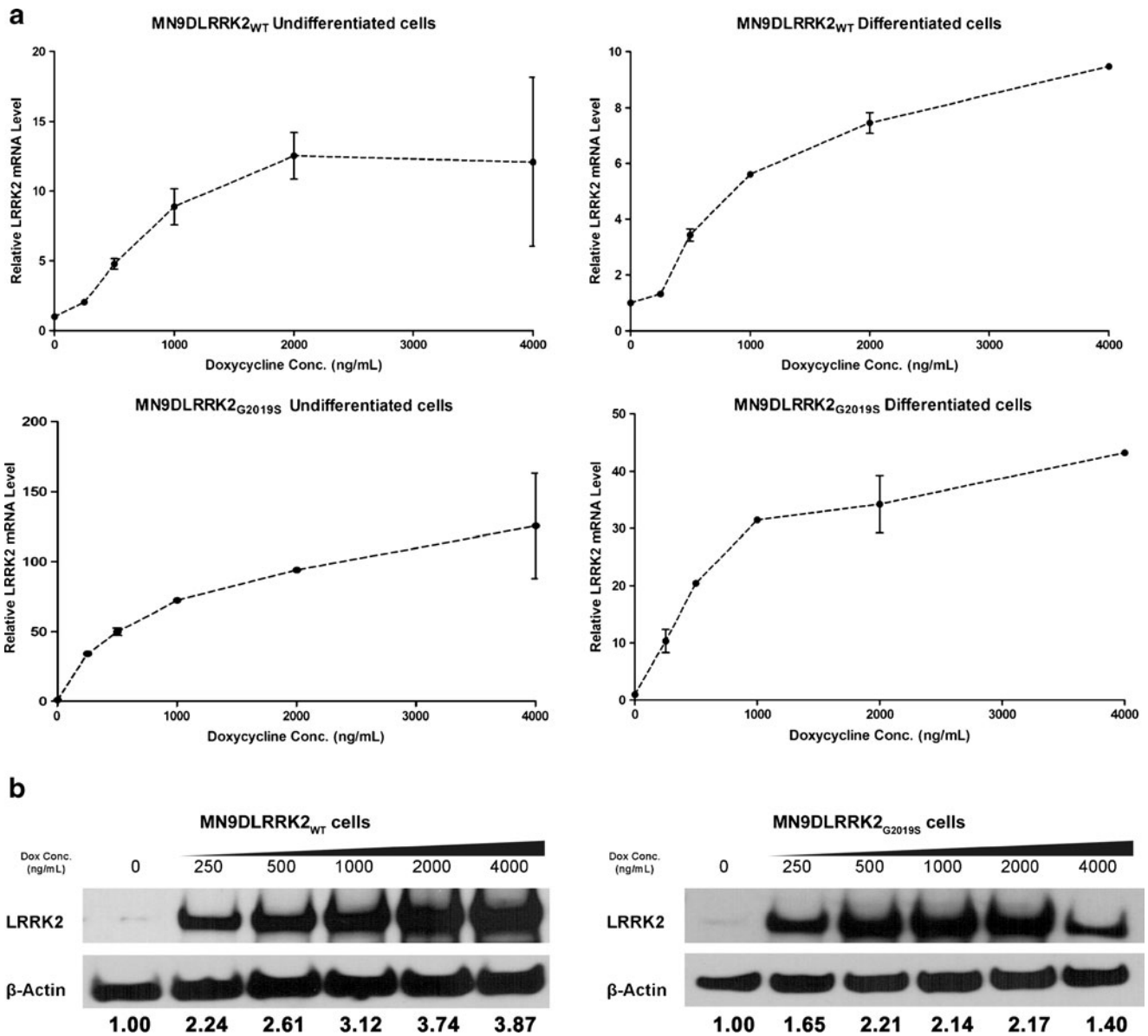

Fig. 1 Doxycycline (DOX)-induced *LRRK2* expression in MN9DLRRK2WT and MN9DLRRK2G2019S cells. DOX was added to the culture media 48 h before harvesting using an RNA/DNA/Protein Purification Kit (Norgen, Thorold, ON, Canada). For differentiated cells, cells were treated with 2 mM sodium butyrate for 6 days before the addition of DOX. **a** Quantitative real-time reverse transcription-polymerase chain reaction was performed to measure LRRK2 messenger RNA (mRNA) levels of DOX-induced undifferentiated and differentiated MN9DLRRK2WT (top panels) or MN9DLRRK2G2019S (bottom panels) cells. **b** Western blot analysis of *LRRK2* expression upon DOX induction. For MN9DLRRK2WT cells, 20 μg of total protein was loaded for each sample; for MN9DLRRK2G2019S cells, 5 μg of total protein was loaded for each sample. β-Actin was used as a loading control. Quantitative determinations of intensities of LRRK2 signals normalized to β-actin were shown at the bottom of the Western blot

JrnlID 13311_ArtID 208_Proof# 1 - 02/08/2013

Q1

DOX over the range of 200–4000 ng/mL. The DOX-induced LRRK2 protein expression in MN9DLRRK2$_{WT}$ cells was also dose-dependent (Fig. 1B, left). Both undifferentiated and differentiated MN9DLRRK2$_{G2019S}$ cells displayed a similar dose-dependent induction of LRRK2 gene and protein expression (Fig. 1A, bottom panels, Fig. 1B, right) as MN9DLRRK2$_{WT}$ cells. However, the induction of LRRK2 mRNA expression in both undifferentiated (Fig. 1A, bottom left) and differentiated MN9DLRRK2$_{G2019S}$ cells (Fig. 1A, bottom right) was much greater than in the MN9DLRRK2$_{WT}$ cells, with approximately 120-fold mRNA induction in undifferentiated and 40-fold induction in differentiated cells in response to DOX. No human or mouse LRRK2 protein was detected in MN9D parental cells, which are of mouse origin, with or without DOX treatment (data not shown).

Cellular Expression Pattern of Human LRRK2 in MN9DLRRK2 Cell Lines

The stably-expressing cell lines were examined for the cellular pattern of human LRRK2 by immunocytochemistry. Stable cell lines grown on coverslips and differentiated to a neuronal phenotype for 6 days with sodium butyrate were either induced with DOX or remained uninduced (no DOX). Forty-eight hours later, cells were subjected to immunocytochemistry staining for human LRRK2. The human LRRK2 (Fig. 2A, red) was detected only in DOX-induced (+), GFP-positive (Fig. 2A, green) MN9DLRRK2$_{WT}$ and MN9DLRRK2$_{G2019S}$ cells (Fig. 2A). The LRRK2 expression appears cytosolic, with little or no nuclear staining. There was no significantly enriched subcellular expression of LRRK2 noted. LRRK2 was also detected in neurites following sodium butyrate differentiation (Fig. 2B). A marked blunting of neurite outgrowth was observed in MN9DLRRK2$_{G2019S}$ expressing cells, a phenotypic feature studied in subsequent experiments (see Fig. 4).

LRRK2 Effects on Cell Viability

The cell viability of MN9DLRRK2$_{WT}$ and MN9DLRRK2$_{G2019S}$ cells following LRRK2 induction only or in combination of the addition of toxicants (MPP+ or lactacystin) were evaluated using a MTS assay. When LRRK2 was induced in the MN9DLRRK2$_{WT}$ cells, viability increased in a DOX dose-dependent manner relative to uninduced cells (Fig. 3A, PBS). When MN9DLRRK2$_{WT}$ were challenged with cytotoxic doses of MPP+ (Fig. 3A, MPP+), LRRK2 WT induction increased cellular viability in a DOX dose-dependent fashion. Cell viability with lactacystin treatment was not different between DOX treatment groups (Fig. 3A, lactacystin). In contrast, DOX induction of mutant LRRK2 expression (MN9DLRRK2$_{G2019S}$) resulted in no changes in cellular viability at baseline or following toxicant challenge (Fig. 3B). Similar results were obtained with the

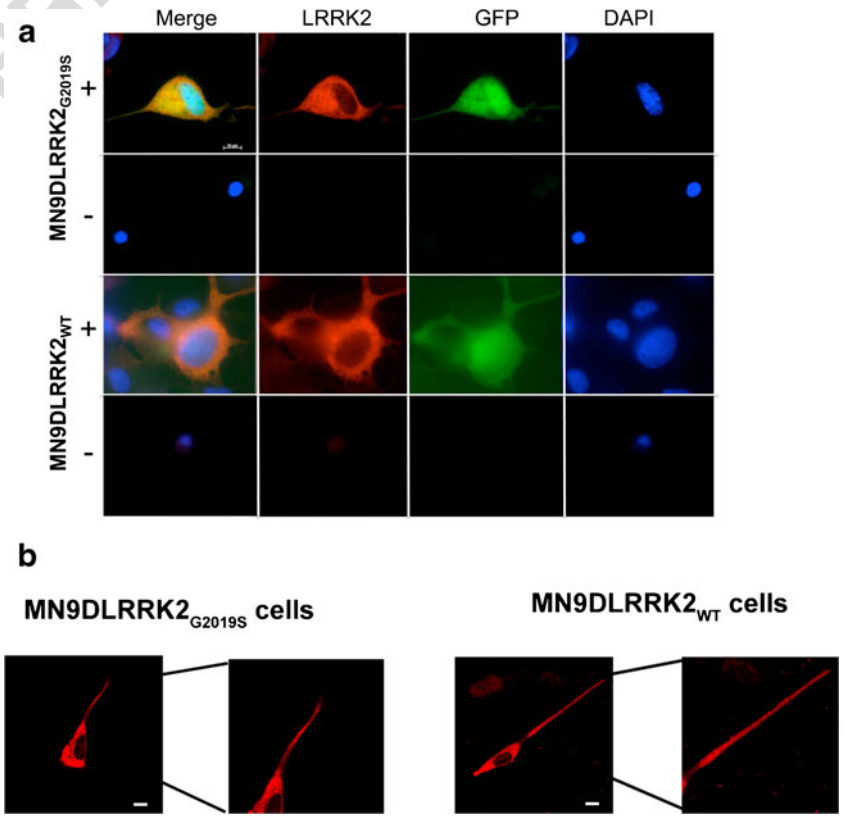

Fig. 2 LRRK2 immunocytochemistry. **a** LRRK2 was detected (*red*) only in doxycycline (DOX) induced (+) green fluorescent protein (GFP) positive (*green*) MN9DLRRK2$_{WT}$ and MN9DLRRK2$_{G2019S}$ cells compared with cells grown in the absence of DOX (−). **b** *LRRK2* was expressed in the neurites of sodium butyrate-differentiated DOX-induced cells. Parts of the image showing the neurites are enlarged to show LRRK2 expression. Image acquisition was with 40× magnification; scale bar is 10 μm. *DAPI* 4',6-diamidino-2-phenylindole

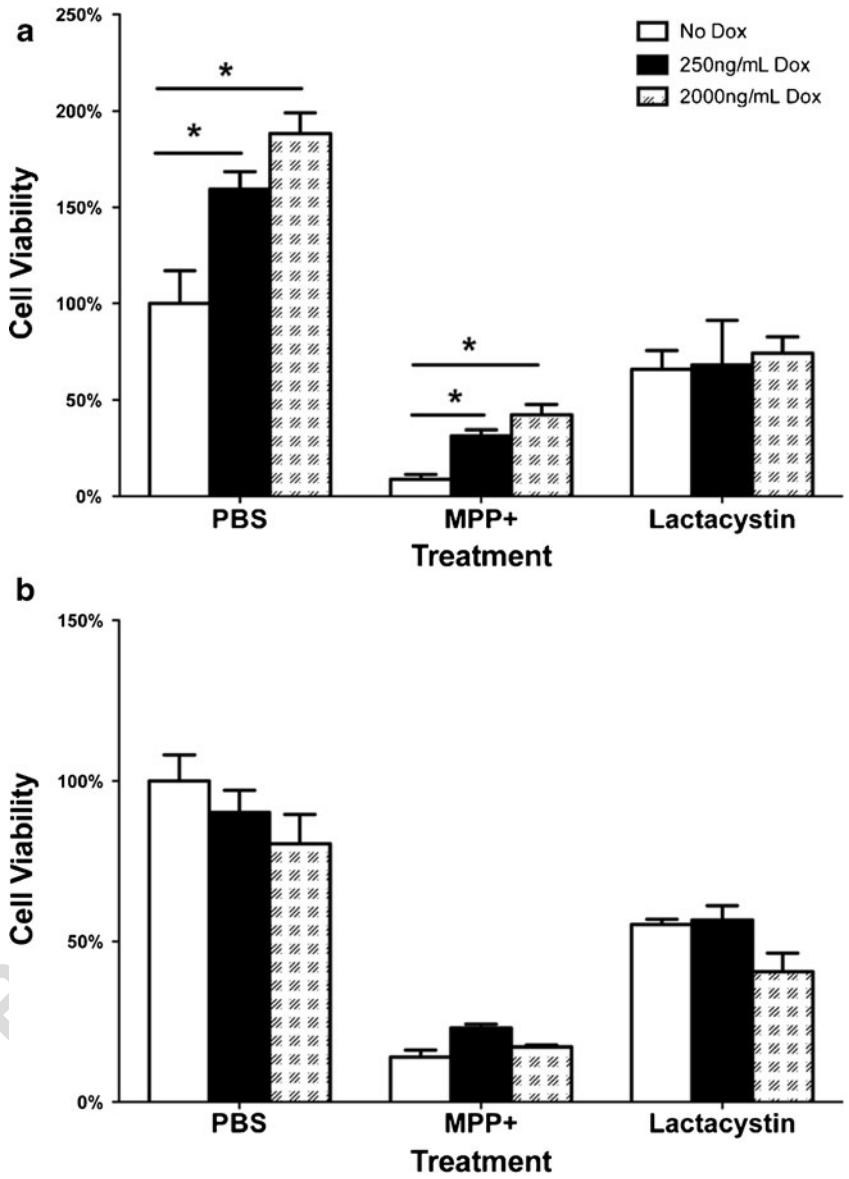

Fig. 3 Cell viability of $MN9DLRRK2_{WT}$ and $MN9DLRRK2_{G2019S}$ lines in response to LRRK2 induction only or in combination with MPP + or lactacystin. **a** $MN9DLRRK2_{WT}$ cells were plated in a 96-well configuration and induced with 250 ng/mL or 2000 ng/mL doxycycline (DOX) for 48 h, followed by incubation with either phosphate buffered saline (PBS), 500 μM MPP + or 5 μM lactacystin. Cell viability was determined by an MTS assay. **b** $MN9D_{G2019S}$ cells were plated in 96-well configuration and induced with 250 ng/mL or 2000 ng/mL DOX for 48 h, followed by incubation with either PBS, 500 μM MPP + or 5 μM lactacystin. Cell viability was determined by an MTS assay. *$p<0.05$ *vs* No DOX; one-way analysis of variance

lactate dehydrogenase cytotoxicity assay (i.e., DOX induction of LRRK2 WT, but not LRRK2 G2019S, increased cellular viability over time (data not shown).

LRRK2 G2019S Expression Blunts Neurite Extension and is Reversed by Treatment With Kinase Inhibitor IN-1

Sodium butyrate-differentiated MN9DLRRK2 cells were induced with DOX and examined for neurite extension (Fig. 4). Quantitative neurite extension was undertaken at 48 (Fig. 4A) and 96 h (Fig. 4B) with (+DOX) or without DOX induction. $MN9DLRRK2_{G2019S}$ (G2019S), but not $MN9DLRRK2_{WT}$ (WT), cells showed a statistically significant blunting of neurite extension only when LRRK2 was induced by DOX. Photomicrographs of MN9D neurites from the different cell lines under the different conditions are shown in Fig. 4C.

A specific and potent kinase inhibitor, IN-1 [38], was examined to determine whether inhibition of LRRK2 G2019S activity would alter the pathobiologic neurite phenotype. We first confirmed that IN-1 would reduce LRRK2 phosphorylation of endogenous serine residues at positions 910 and 935 (Fig. 5A). As anticipated, phosphorylation of both sites was reduced in an IN-1 concentration-dependent manner. Following immunocytochemistry for beta-tubulin III, we noted that blunted neurite extension mediated by LRRK2 G2019S overexpression was rescued by IN-1 treatment (Fig. 5B). Quantitative neurite extension studies confirmed the morphological changes and showed that the blunted neuritic phenotype was abrogated by

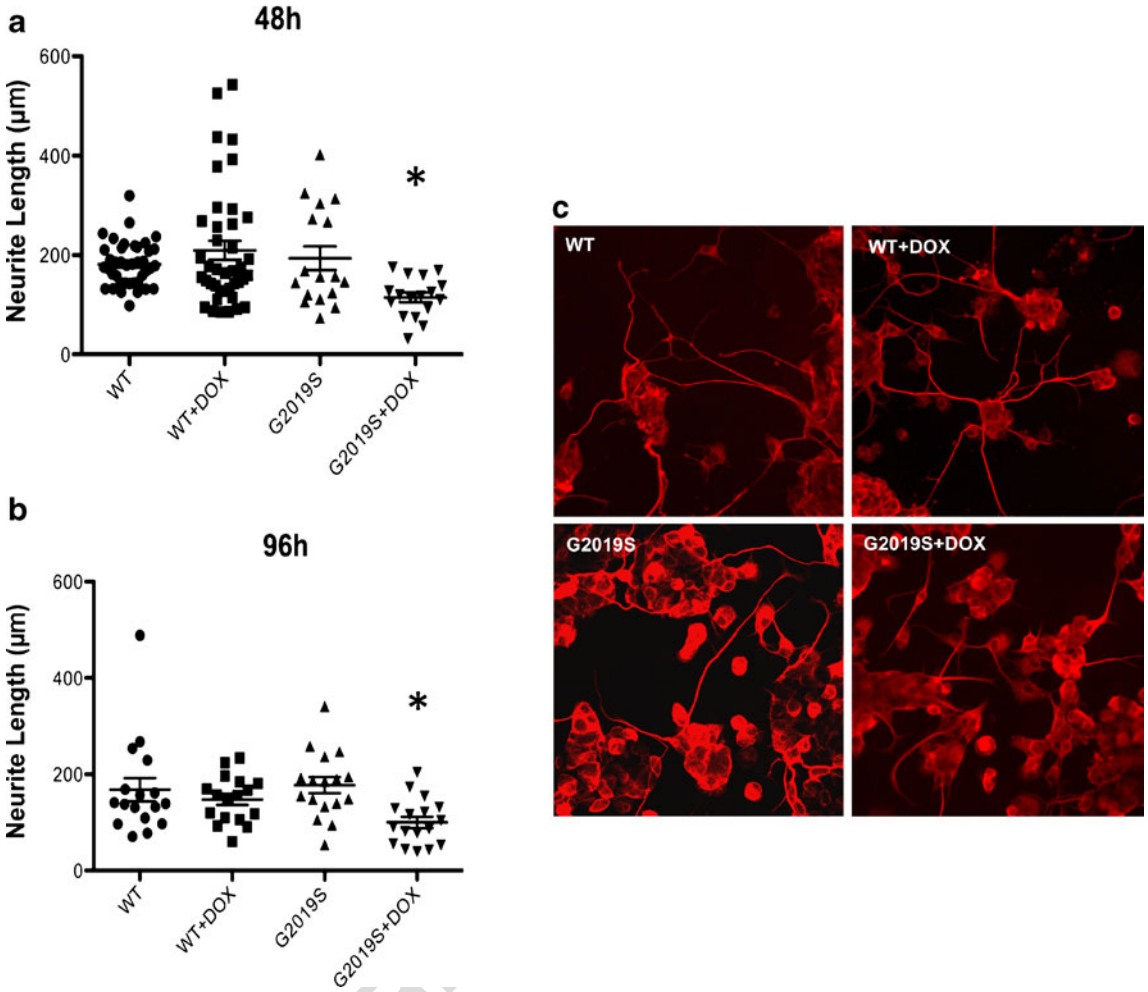

Fig. 4 Neurite length is shortened in MN9DLRRK2$_{G2019S}$ cells with doxycycline (DOX) induction of LRRK2 G2019S. MN9DLRRK2$_{WT}$ or MN9DLRRK2$_{G2019S}$ cells were plated on polyethylenemine-coated 12-mm coverslips in a 24-well plate and differentiated with 2 mM sodium butyrate for 6 days. DOX (250 ng/mL) was added to the cells to induce LRRK2 expression for 48 h (**a**) or 96 h (**b**). Cells were fixed and immunocytochemically stained for β-tubulin. For each coverslip, pictures of 8 fields were taken and lengths of all neurites were measured with Nikon NIS Elements software. *$p<0.05$ *vs* control; one-way analysis of variance. **c** Representative images of differentiated MN9DLRRK2$_{WT}$ or MN9DLRRK2$_{G2019S}$ cells with [wild-type (WT) + DOX, G2019S+-DOX] or without (WT, G2019S) DOX induction are presented

IN-1 at both 100 and 500 nM. These data demonstrate that MN9DLRRK2$_{G2019S}$ cells have an (DOX) inducible neuritic phenotype (i.e., shorter length) that can be largely reversed by a potent and specific inhibitor of LRRK2, IN-1.

LRRK2 G2019S Mediated Blunting of Neurite Length is Reversed by Allele-Specific RNAi

Undifferentiated and differentiated MN9DLRRK2 cells were transduced with lentiviral constructs (multiplicity of infection=50) expressing a shRNA directed against the G2019S allele (p4) or a sequence scrambled control. PBS treatment was also included as a control for lentivirus transduction. In both undifferentiated and differentiated MN9DLRRK2$_{G2019S}$ cells lentiviral transduction of allele-specific p4, but not the control scrambled sequence, resulted in decreased expression of LRRK2 G2019S messenger RNA (mRNA) (Fig. 6A). By contrast, p4 transduction of MN9DLRRK2$_{WT}$ produced no significant decline in LRRK2 WT mRNA content in either undifferentiated or differentiated cells (Fig. 6B). Furthermore, the allele-specific knockdown of *G2019S* gene product led to a decrease in LRRK2 protein expression in MN9DLRRK2$_{G2019S}$ (Fig. 6C), but not in MN9DLRRK2$_{WT}$ cells (Fig. 6D). In addition, the LRRK2 phosphorylation at amino acids 910 and 935 was decreased in p4 transduced MN9DLRRK2$_{G2019S}$ (Fig. 6E), but not in the MN9DLRRK2$_{WT}$ cells (Fig. 6F). Last, we addressed whether lentiviral transduction could reverse the blunted neuritic phenotype engendered by LRRK2 G2019S induction. As shown in Fig. 6G, transduction with lentiviral p4 shRNA, but not the scrambled shRNA, reversed the neuritic shortening in DOX-induced differentiated MN9DLRRK2$_{G2019S}$ cells.

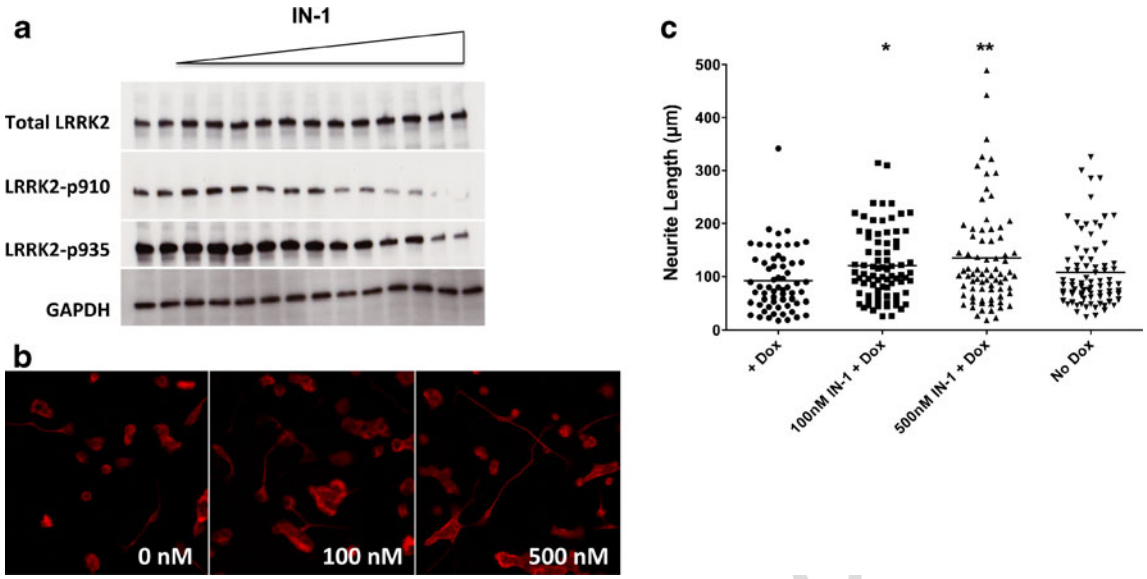

Fig. 5 Evaluation of the LRRK2 inhibitor, IN-1, in MN9DLRRK2$_{G2019S}$ cells. **a** The LRRK2 inhibitor IN-1 decreases LRRK2 phosphorylation at amino acids 910 and 935. MN9DLRRK2$_{G2019S}$ cells were treated with kinase inhibitor IN-1 at various concentrations (30, 100, 300, and 3000 nM) for 90 mins followed by Western blot analysis of total LRRK2, phosphor-LRRK2 at 910 and 935 expression. Equal amounts of total protein were loaded for each sample. **b** Neurite length shortening is reversed in MN9DLRRK2$_{G2019S}$ cells with the addition of the LRRK2 inhibitor IN-1. MN9DLRRK2$_{G2019S}$ cells were plated on polyethylenemine-coated 12-mm coverslips in a 24-well plate and differentiated with 2 mM sodium butyrate for 6 days. Doxycycline (DOX) (250 ng/mL) was added to the cells to induce LRRK2 G2019S expression for 48 h followed by the addition of IN-1 (100 nM or 500 nM). Twenty-four hours later, cells were fixed and immunocytochemically stained for β-tubulin. Representative images are presented for the IN-1 treatment at the concentration of 0 (+DOX), 100 nM and 500 nM. **c** Quantitative measurements of neurite lengths of MN9DLRRK2$_{G2019S}$ cells. For each coverslip, pictures of 8 fields were taken and lengths of all neurites were measured using Nikon NIS Elements software. MN9DLRRK2$_{G2019S}$ without DOX induction (no DOX) was used as a control. *$p<0.05$ *vs* control; **$p<0.01$ *vs* control; one-way analysis of variance. *GAPDH* glyceraldehyde 3-phosphate dehydrogenase

Discussion

The MN9DLRRK2 cell lines described herein can be used to study LRRK2 biology and serve as a cellular platform for LRRK2 therapeutics development. In the case of PD, there have been several LRRK2 animal models reported that include animals from invertebrates to nonhuman primates [44]; however, none demonstrate the progressive degenerative features of human PD. Such animal models may be useful for examination of specific questions of gene product function and/or disease pathogenesis, but appear limited in that they do not recapitulate the many features of PD. To initiate therapeutics development it is optimal to have a model where the cellular content of a putatively pathogenic mutant gene product can be compared across a range of steady-state levels. In addition, a comparator line harboring the nonmutant or WT version of the same gene product is ideal to ensure that the pathophysiology attributed to the mutant gene product can be distinguished, if possible, from that due to expression of the WT form.

Human LRRK2 PD-associated mutations are manifest as autosomal dominant [4], and account for a substantial proportion of familial PD and also are implicated in sporadic PD [5–10]. Additionally, genome-wide association studies studies have identified a single nucleotide polymorphism closely linked to the LRRK2 locus, suggesting a potential role in sporadic/idiopathic PD [45]. LRRK2-targeted therapeutics development appears to be a promising avenue for the potential treatment of symptomatic G2019S gene carriers. In some studies mutant LRRK2, particularly G2019S, is cytotoxic when over-expressed in cultured cells [18, 46], *Drosophila* [30, 47], *Caenorhabditis elegans* [12], and viral vector transduced mice [21]; however, no apparent neuronal loss was observed in transgenic mice carrying LRRK2 mutant genes alone [48–50]. This discordance raises the question as to what levels of *LRRK2* gene product are most relevant for the study of PD pathogenesis and also for therapeutics development.

In our study, we generated inducible stable cell lines expressing *LRRK2 G2019S*, using a previously reported bicistronic and auto-regulated stable transfection strategy [39–41]. The parental MN9D cell line used to make inducible stable cell lines was selected because of its dopaminergic properties when differentiated [51] and because its murine origins allow for the detection, with appropriate Abs, of introduced genes expressing human LRRK2. We studied the following characteristics of the MN9DLRRK2 stably transfected cell lines: LRRK2 expression at the mRNA and protein levels, lactate dehydrogenase release, MTS reduction cell viability, cellular morphology,

Q1

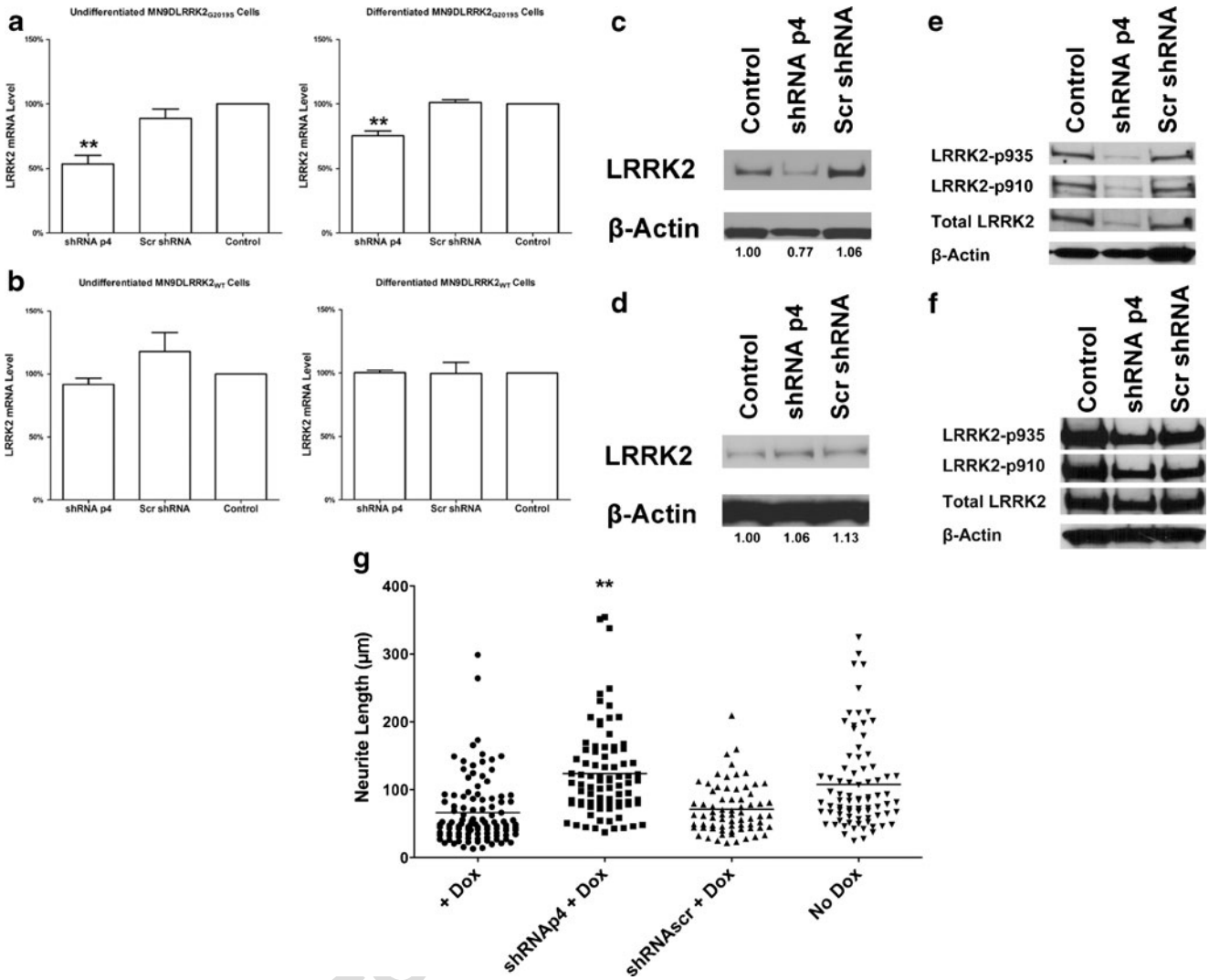

Q11 **Fig. 6** Evaluation of small hairpin RNA (shRNA)p4-mediated allele specific knockdown of LRRK2 G2019S in MN9DLRRK2$_{G2019S}$ cells. **a** The shRNAp4, but not scrambled shRNA (Scr shRNA), significantly decreased LRRK2 G2019S messenger RNA (mRNA) levels in both undifferentiated and differentiated MN9DLRRK2$_{G2019S}$ cells. Only the shRNAp4 exhibited a significant decrease in LRRK2 mRNA level [$^{**}p<0.01$, one-way analysis of variance (ANOVA)]. Cell differentiation was induced by treating MN9DLRRK2$_{G2019S}$ cells with 2 mM sodium butyrate for 6 days before transduction. Cells were then processed in the same way as undifferentiated cells. Similar to undifferentiated cells, only the shRNA p4 exhibited significant decrease in LRRK2 mRNA level ($^{**}p<0.01$ one-way ANOVA). **b** The shRNAp4 did not inhibit wild-type (WT) LRRK2 expression. No significant difference in LRRK2 mRNA level was observed in these experimental groups. Error bars indicate the standard error of the mean and represent 3 independent experiments. **c** Western blot showing a decrease of LRRK2 G2019S protein in Lenti-shRNAp4-transduced MN9DLRRK2$_{G2019S}$ cells. β-Actin is used as a loading control. Quantitative determinations of intensities of LRRK2 signals normalized to β-actin were shown at the bottom of the Western blot. **d** Western blot showing no change of WT LRRK2 protein in lenti-shRNAp4-transduced MN9DLRRK2$_{WT}$ cells. β-Actin is used as a loading control. Quantitative determinations of intensities of LRRK2 signals normalized to β-actin were shown at the bottom of the Western blot. **e** Western blot showing decreases of LRRK2 phosphorylation at amino acids 910 and 935 in lenti-shRNAp4-transduced MN9DLRRK2$_{G2019S}$ cells, but not in (**f**) MN9DLRRK2$_{WT}$ cells. **g** Neurite length shortening is reversed in MN9D$_{G2019S}$ cells following lenti-shRNAp4 transduction. MN9DLRRK2$_{G2019S}$ cells were plated on polyethylenemine-coated 12-mm coverslips in a 24-well plate and differentiated with 2 mM sodium butyrate for 6 days. Forty-eight hours before transduction, doxycycline (DOX) (250 ng/mL) was added to the cells to induce LRRK2 G2019S expression. Seventy-two hours after transduction, cells were fixed and immunocytochemically stained for β-tubulin. For each coverslip, pictures of 8 fields were taken and lengths of all neurites were measured using Nikon NIS Elements software. MN9DLRRK2$_{G2019S}$ without DOX induction (no DOX) was used as a control. $^{**}p<0.01$ *vs* control; one-way ANOVA

LRRK2 interaction with toxicants MPP + and lactacystin, effects of LRRK2 kinase inhibitor treatment, and effects of LRRK2 G2019S allele-specific shRNA gene knockdown.

We showed that increased expression of WT LRRK2 in MN9DLRRK2$_{WT}$ cells caused an apparent increase in cell viability. No significant change in cell viability was observed

when LRRK2 was induced in MN9DLRRK2$_{G2019}$ cells. When MN9DLRRK2$_{WT}$ cells were challenged with MPP + there was significant decline in cell viability in the absence of LRRK2 induction and, interestingly, cell viability significantly increased when LRRK2 was induced. MPP + treatment produced substantial decline in cell viability in MN9DLRRK2$_{G2019S}$ cells that was not ameliorated by the induction of LRRK2. It appeared that LRRK2 WT provided protection against a neurotoxin that caused mitochondrial dysfunction. These observations were in line with the recent *C. elegans* study, which showed that LRRK2 WT, but not LRRK2 mutant, protected dopaminergic neurons against rotenone or paraquat toxicity, agents which compromise [52]. The underlying mechanisms by which LRRK2 WT protected mitochondrial dysfunction remained to be determined. The MN9DLRRK2 cell models enable further studies on the association of LRRK2 action and mitochondrial function. In both MN9DLRRK2$_{WT}$ and MN9DLRRK2$_{G2019S}$ cells treatment with lactacystin, a proteosomal inhibitor, caused a decline in cell viability that was unaffected by induction of either WT or G2019S mutant LRRK2, suggesting that in the MN9D cellular context LRRK2 does not affect proteosome function.

We also studied the effect of LRRK2 expression on MN9D neurite outgrowth after differentiation with sodium butyrate. As reported by other investigators in different cell types [53–59], we also observed that the overexpression of *LRRK2 G2019S* results in shortened neuritic extensions. We explored potential molecular contributors to this pathogenic neuritic phenotype. We sought to determine whether ERM phosphorylation may be involved given that in *LRRK2 G2019S* transgenic hippocampal neurons axonal length was reduced and required increased ERM phosphorylation [58]. However, in differentiated and DOX-induced MN9DLRRK2$_{G2019S}$ cells no change in overall ERM or ERM phosphorylation levels were observed (data not shown). Unlike primary hippocampal neurons that manifest marked axonal and dendritic features, MN9D neurites are less functionally specified [51]. Whether neurite blunting, which occurs in the absence of MN9DLRRK2$_{G2019S}$ cell death, is due to specific changes that alter the cytoskeleton and/or produce metabolic dysfunction is not known.

One of the goals for construction of the LRRK2 MN9D cell lines was to study candidate therapeutic strategies directed against the LRRK2 target. The G2019S mutant form of LRRK2 conveys an increase in kinase activity compared with the WT [13, 18, 23, 29, 30, 46, 60–63]. Not surprisingly, the causal role of dysregulated kinase activity of G2019S has spawned interest in the development of kinase inhibitors, which, if potent and specific, represent disease-modifying therapeutics for PD patients harboring the *LRRK2 G2019S* allele. One pharmacophore, IN-1 kinase inhibitor, was described by Deng et al. [38] as having an IC_{50} in the low nM range and high specificity for LRRK2 [38]. We evaluated IN-1 in both MN9DLRRK2$_{WT}$ and MN9DLRRK2$_{G2019S}$ cell lines. The data indicate that IN-1 does inhibit LRRK2 phosphorylation at both S910 and S935 without affecting the levels of total LRRK2 protein. In addition, we tested whether LRRK2 G2019S inhibition would reverse the pathogenic action of dysregulated kinase activity. Our observations indicate that this was, indeed, the case. Notably, IN-1 reversed the neurite blunting phenotype in a dose-dependent manner. The literature suggests that S910 and S935 are autophosphorylation sites on LRRK2 [64–66], although recent work reveals that S1292, at least in some cellular contexts, is also a pathogenically relevant LRRK2 autophophosphorylation site [34]. The IN-1 dose-dependent reduction of phosphoserine residues on LRRK2 in both cell lines support their use in the prosecution of small molecule kinase inhibitors. The ability to independently modulate LRRK2 levels during cell-based drug discovery efforts is another advantage of the MN9DLRRK2 cell lines in that LRRK2-mediated pathophysiological effects, and kinase inhibitor interdiction, may be more readily discovered at particular steady-state levels of LRRK2.

The MN9DLRRK2$_{G2019S}$ cell line was also used to evaluate LRRK2 transcript knockdown promoted by lentiviral transduction of shRNAs targeting the mutant allele. The results indicate that the p4 shRNA was effective in decreasing G2019S mRNA and protein levels in both undifferentiated and differentiated MN9DLRRK2$_{G2019S}$ cells. In addition, we showed that p4 was allele specific as it did not decrease WT LRRK2 expression. Most importantly, the neurite blunting phenotype engendered by *LRRK2 G2019S* was reversed by lentiviral p4 transduction. Prior work using RNA interference, introduced by transient transfection, has made evident that the G2019S target sequence, when embedded in a synthetic substrate, can be effectively targeted relative to WT sequence [43]. Our results with shRNA transduced by lentiviral vector are, to our knowledge, the first demonstration of allele selective knockdown of a native G2019S transcript and, importantly, the reduction in mutant gene product levels. This finding portends the rapid extrapolation of these constructs into an *in vivo* model.

Our key finding, blunted neurites upon G2019S induction without cytotoxicity, is in agreement with other reported results. Dächsel et al. [59] observed that expression of the G2019S mutant in primary neurons from transgenic mice resulted in diminished neurite outgrowth and branching [59]. Similarly, in transfected primary rat cortical neurons the forced expression of LRRK2 G2019S also resulted in neuritic shortening [56]. In MN9D cells, the induction of mutant G2019S gene does not cause cytotoxicity. While other investigators have reported toxicity when LRRK2 is overexpressed this may be function of the levels of gene product. In our stably transfected MN9DLRRK2$_{G2019S}$ cell line we observed a greater than 40-fold increase in transcript level and marked elevation of gene product. Unlike transiently transfected cells

these MN9DLRRK2$_{G2019S}$ cells are selected for an integrated transgene and expanded in the absence of DOX. Whether this process of cell line construction or, alternatively, the nature of fusion cell line account for the absence of G2019S toxicity is unknown.

Our inducible stable MN9D cell lines appear useful for the study of LRRK2 biology in the context of a dopaminergic background and over a range of gene product levels. The absence of cytotoxicity and presence of a neuritic blunting phenotype in the MN9DLRRK2$_{G2019S}$ cells enable their use for the evaluation of candidate therapeutics, small molecule kinase inhibitors, and also RNA interference strategies.

Acknowledgments This work was supported RC2NS069450 (NIH/NINDS/ARRA) to HJF and DOD grant USAMRMC11341009 to HJF. We thank Dr. M. Cookson and Ms. A. Kaganovich from NIA/NIH (Bethesda, MD, USA) for their valuable technical advice on neurite assay, and Amanda Edwards for her help with the evaluation of the cell lines.

Required Author Forms Disclosure forms provided by the authors are available with the online version of this article.

References

1. Zimprich A, Biskup S, Leitner P, Lichtner P, Farrer M, Lincoln S, et al. Mutations in LRRK2 cause autosomal-dominant parkinsonism with pleomorphic pathology. Neuron 2004;44:601–607.
2. Paisan-Ruiz C, Lang AE, Kawarai T, Sato C, Salehi-Rad S, Fisman GK, et al. LRRK2 gene in Parkinson disease: mutation analysis and case control association study. Neurology 2005;65:696–700.
3. Paisan-Ruiz C, Jain S, Evans EW, Gilks WP, Simon J, van der Brug M, et al. Cloning of the gene containing mutations that cause PARK8-linked Parkinson's disease. Neuron 2004;44:595–600.
4. Funayama M, Hasegawa K, Kowa H, Saito M, Tsuji S, Obata F. A new locus for Parkinson's disease (PARK8) maps to chromosome 12p11.2-q13.1. Ann Neurol 2002;51:296–301.
5. Zabetian CP, Samii A, Mosley AD, Roberts JW, Leis BC, Yearout D, et al. A clinic-based study of the LRRK2 gene in Parkinson disease yields new mutations. Neurology 2005;65:741–744.
6. Tan EK, Skipper LM. Pathogenic mutations in Parkinson disease. Hum Mutat 2007;28:641–653.
7. Nichols WC, Pankratz N, Hernandez D, Paisan-Ruiz C, Jain S, Halter CA, et al. Genetic screening for a single common LRRK2 mutation in familial Parkinson's disease. Lancet 2005;365:410–412.
8. Gilks WP, Abou-Sleiman PM, Gandhi S, Jain S, Singleton A, Lees AJ, et al. A common LRRK2 mutation in idiopathic Parkinson's disease. Lancet 2005;365:415–416.
9. Farrer M, Stone J, Mata IF, Lincoln S, Kachergus J, Hulihan M, et al. LRRK2 mutations in Parkinson disease. Neurology 2005;65:738–40.
10. Di Fonzo A, Rohe CF, Ferreira J, Chien HF, Vacca L, Stocchi F, et al. A frequent LRRK2 gene mutation associated with autosomal dominant Parkinson's disease. Lancet 2005;365:412–415.
11. Hardy J. Genetic analysis of pathways to Parkinson disease. Neuron 2010;68:201–6.
12. Li X, Tan YC, Poulose S, Olanow CW, Huang XY, Yue Z. Leucine-rich repeat kinase 2 (LRRK2)/PARK8 possesses GTPase activity that is altered in familial Parkinson's disease R1441C/G mutants. J Neurochem 2007;103:238–247.
13. West AB, Moore DJ, Choi C, Andrabi SA, Li X, Dikeman D, et al. Parkinson's disease-associated mutations in LRRK2 link enhanced GTP-binding and kinase activities to neuronal toxicity. Hum Mol Genet 2007;16:223–232.
14. Mata IF, Wedemeyer WJ, Farrer MJ, Taylor JP, Gallo KA. LRRK2 in Parkinson's disease: protein domains and functional insights. Trends Neurosci 2006;29:286–293.
15. Biskup S, West AB. Zeroing in on LRRK2-linked pathogenic mechanisms in Parkinson's disease. Biochim Biophys Acta 2009;1792:625–633.
16. Tsika E, Moore DJ. Mechanisms of LRRK2-mediated neurodegeneration. Curr Neurol Neurosci Rep 2012;12:251–260.
17. Hernandez D, Paisan Ruiz C, Crawley A, Malkani R, Werner J, Gwinn-Hardy K, et al. The dardarin G 2019 S mutation is a common cause of Parkinson's disease but not other neurodegenerative diseases. Neurosci Lett 2005;389:137–139.
18. Greggio E, Jain S, Kingsbury A, Bandopadhyay R, Lewis P, Kaganovich A, et al. Kinase activity is required for the toxic effects of mutant LRRK2/dardarin. Neurobiol Dis 2006;23:329–341.
19. Smith WW, Pei Z, Jiang H, Moore DJ, Liang Y, West AB, et al. Leucine-rich repeat kinase 2 (LRRK2) interacts with parkin, and mutant LRRK2 induces neuronal degeneration. Proc Natl Acad Sci U S A 2005;102:18676–18681.
20. Cookson MR. The role of leucine-rich repeat kinase 2 (LRRK2) in Parkinson's disease. Nat Rev Neurosci 2010;11:791–797.
21. Lee BD, Shin JH, VanKampen J, Petrucelli L, West AB, Ko HS, et al. Inhibitors of leucine-rich repeat kinase-2 protect against models of Parkinson's disease. Nat Med 2010;16:998–1000.
22. Ohta E, Kawakami F, Kubo M, Obata F. LRRK2 directly phosphorylates Akt1 as a possible physiological substrate: impairment of the kinase activity by Parkinson's disease-associated mutations. FEBS Lett 2011;585:2165–170.
23. West AB, Moore DJ, Biskup S, Bugayenko A, Smith WW, Ross CA, et al. Parkinson's disease-associated mutations in leucine-rich repeat kinase 2 augment kinase activity. Proc Natl Acad Sci U S A 2005;102:16842–16847.
24. Gloeckner CJ, Kinkl N, Schumacher A, Braun RJ, O'Neill E, Meitinger T, et al. The Parkinson disease causing LRRK2 mutation I2020T is associated with increased kinase activity. Hum Mol Genet 2006;15:223–232.
25. Hsu CH, Chan D, Greggio E, Saha S, Guillily MD, Ferree A, et al. MKK6 binds and regulates expression of Parkinson's disease-related protein LRRK2. J Neurochem 2010;112:1593–1604.
26. Ito G, Okai T, Fujino G, Takeda K, Ichijo H, Katada T, et al. GTP binding is essential to the protein kinase activity of LRRK2, a causative gene product for familial Parkinson's disease. Biochemistry 2007;46:1380–1388.
27. Kamikawaji S, Ito G, Iwatsubo T. Identification of the autophosphorylation sites of LRRK2. Biochemistry 2009;48:10963–10975.
28. Li X, Moore DJ, Xiong Y, Dawson TM, Dawson VL. Reevaluation of phosphorylation sites in the Parkinson disease-associated leucine-rich repeat kinase 2. J Biol Chem 2010;285:29569–29576.
29. Jaleel M, Nichols RJ, Deak M, Campbell DG, Gillardon F, Knebel A, et al. LRRK2 phosphorylates moesin at threonine-558: characterization of how Parkinson's disease mutants affect kinase activity. Biochem J 2007;405:307–317.
30. Imai Y, Gehrke S, Wang HQ, Takahashi R, Hasegawa K, Oota E, et al. Phosphorylation of 4E-BP by LRRK2 affects the maintenance of dopaminergic neurons in Drosophila. EMBO J 2008;27:2432–2443.
31. Gandhi PN, Wang X, Zhu X, Chen SG, Wilson-Delfosse AL. The Roc domain of leucine-rich repeat kinase 2 is sufficient for interaction with microtubules. J Neurosci Res 2008;86:1711–1720.
32. Gloeckner CJ, Schumacher A, Boldt K, Ueffing M. The Parkinson disease-associated protein kinase LRRK2 exhibits MAPKKK activity and phosphorylates MKK3/6 and MKK4/7, in vitro. J Neurochem 2009;109:959–968.

33. Kumar A, Greggio E, Beilina A, Kaganovich A, Chan D, Taymans JM, et al. The Parkinson's disease associated LRRK2 exhibits weaker in vitro phosphorylation of 4E-BP compared to autophosphorylation. PLoS One 2010;5:e8730.
34. Sheng Z, Zhang S, Bustos D, Kleinheinz T, Le Pichon CE, Dominguez SL, et al. Ser1292 autophosphorylation is an indicator of LRRK2 kinase activity and contributes to the cellular effects of PD mutations. Sci Transl Med 2012;4:164ra1.
35. Lesage S, Durr A, Tazir M, Lohmann E, Leutenegger AL, Janin S, et al. LRRK2 G2019S as a cause of Parkinson's disease in North African Arabs. N Engl J Med 2006;354:422–423.
36. Saunders-Pullman R, Lipton RB, Senthil G, Katz M, Costan-Toth C, Derby C, et al. Increased frequency of the LRRK2 G2019S mutation in an elderly Ashkenazi Jewish population is not associated with dementia. Neurosci Lett 2006;402:92–96.
37. Ozelius LJ, Senthil G, Saunders-Pullman R, Ohmann E, Deligtisch A, Tagliati M, et al. LRRK2 G2019S as a cause of Parkinson's disease in Ashkenazi Jews. N Engl J Med 2006;354:424–425.
38. Deng X, Dzamko N, Prescott A, Davies P, Liu Q, Yang Q, et al. Characterization of a selective inhibitor of the Parkinson's disease kinase LRRK2. Nat Chem Biol 2011;7:203–205.
39. Su X, Maguire-Zeiss KA, Giuliano R, Prifti L, Venkatesh K, Federoff HJ. Synuclein activates microglia in a model of Parkinson's disease. Neurobiol Aging 2008;29:1690–1701.
40. Strathdee CA, McLeod MR, Hall JR. Efficient control of tetracycline-responsive gene expression from an autoregulated bi-directional expression vector. Gene 1999;229:21–29.
41. Luo Y, Henricksen LA, Giuliano RE, Prifti L, Callahan LM, Federoff HJ. VIP is a transcriptional target of Nurr1 in dopaminergic cells. Exp Neurol 2007;203:221–232.
42. Choi HK, Won LA, Kontur PJ, Hammond DN, Fox AP, Wainer BH, et al. Immortalization of embryonic mesencephalic dopaminergic neurons by somatic cell fusion. Brain Res 1991;552:67–76.
43. Sibley CR, Wood MJ. Identification of allele-specific RNAi effectors targeting genetic forms of Parkinson's disease. PLoS One 2011;6:e26194.
44. Dawson TM, Ko HS, Dawson VL. Genetic animal models of Parkinson's disease. Neuron 2010;66:646–661.
45. Liu X, Cheng R, Verbitsky M, Kisselev S, Browne A, Mejia-Sanatana H, et al. Genome-wide association study identifies candidate genes for Parkinson's disease in an Ashkenazi Jewish population. BMC Med Genet 2011;12:104.
46. Smith WW, Pei Z, Jiang H, Dawson VL, Dawson TM, Ross CA. Kinase activity of mutant LRRK2 mediates neuronal toxicity. Nat Neurosci 2006;9:1231–1233.
47. Liu Z, Wang X, Yu Y, Li X, Wang T, Jiang H, et al. A Drosophila model for LRRK2-linked parkinsonism. Proc Natl Acad Sci U S A 2008;105:2693–2698.
48. Li Y, Liu W, Oo TF, Wang L, Tang Y, Jackson-Lewis V, et al. Mutant LRRK2(R1441G) BAC transgenic mice recapitulate cardinal features of Parkinson's disease. Nat Neurosci 2009;12:826–828.
49. Tong Y, Pisani A, Martella G, Karouani M, Yamaguchi H, Pothos EN, et al. R1441C mutation in LRRK2 impairs dopaminergic neurotransmission in mice. Proc Natl Acad Sci U S A 2009;106:14622–14627.
50. Lin X, Parisiadou L, Gu XL, Wang L, Shim H, Sun L, et al. Leucine-rich repeat kinase 2 regulates the progression of neuropathology induced by Parkinson's-disease-related mutant alpha-synuclein. Neuron 2009;64:807–827.
51. Choi HK, Won L, Roback JD, Wainer BH, Heller A. Specific modulation of dopamine expression in neuronal hybrid cells by primary cells from different brain regions. Proc Natl Acad Sci U S A 1992;89:8943–8947.
52. Saha S, Guillily MD, Ferree A, Lanceta J, Chan D, Ghosh J, et al. LRRK2 modulates vulnerability to mitochondrial dysfunction in Caenorhabditis elegans. J Neurosci 2009;29:9210–9218.
53. Winner B, Melrose HL, Zhao C, Hinkle KM, Yue M, Kent C, et al. Adult neurogenesis and neurite outgrowth are impaired in LRRK2 G2019S mice. Neurobiol Dis 2011;41:706–716.
54. Ramonet D, Daher JP, Lin BM, Stafa K, Kim J, Banerjee R, et al. Dopaminergic neuronal loss, reduced neurite complexity and autophagic abnormalities in transgenic mice expressing G2019S mutant LRRK2. PLoS One 2011;6:e18568.
55. Plowey ED, Cherra SJ, 3rd, Liu YJ, Chu CT. Role of autophagy in G2019S-LRRK2-associated neurite shortening in differentiated SH-SY5Y cells. J Neurochem 2008;105:1048–1056.
56. MacLeod D, Dowman J, Hammond R, Leete T, Inoue K, Abeliovich A. The familial Parkinsonism gene LRRK2 regulates neurite process morphology. Neuron 2006;52:587–593.
57. Heo HY, Kim KS, Seol W. Coordinate regulation of neurite outgrowth by LRRK2 and its interactor, Rab5. Exp Neurobiol 2010;19:97–105.
58. Parisiadou L, Xie C, Cho HJ, Lin X, Gu XL, Long CX, et al. Phosphorylation of ezrin/radixin/moesin proteins by LRRK2 promotes the rearrangement of actin cytoskeleton in neuronal morphogenesis. J Neurosci 2009;29:13971–13980.
59. Dachsel JC, Behrouz B, Yue M, Beevers JE, Melrose HL, Farrer MJ. A comparative study of Lrrk2 function in primary neuronal cultures. Parkinsonism Relat Disord 2010;16:650–655.
60. Luzon-Toro B, Rubio de la Torre E, Delgado A, Perez-Tur J, Hilfiker S. Mechanistic insight into the dominant mode of the Parkinson's disease-associated G2019S LRRK2 mutation. Hum Mol Genet 2007;16:2031–2039.
61. Guo L, Gandhi PN, Wang W, Petersen RB, Wilson-Delfosse AL, Chen SG. The Parkinson's disease-associated protein, leucine-rich repeat kinase 2 (LRRK2), is an authentic GTPase that stimulates kinase activity. Exp Cell Res 2007;313:3658–3670.
62. Covy JP, Giasson BI. Identification of compounds that inhibit the kinase activity of leucine-rich repeat kinase 2. Biochem Biophys Res Commun 2009;378:473–477.
63. Anand VS, Reichling LJ, Lipinski K, Stochaj W, Duan W, Kelleher K, et al. Investigation of leucine-rich repeat kinase 2: enzymological properties and novel assays. FEBS J 2009;276:466–478.
64. Nichols RJ, Dzamko N, Morrice NA, Campbell DG, Deak M, Ordureau A, et al. 14-3-3 binding to LRRK2 is disrupted by multiple Parkinson's disease-associated mutations and regulates cytoplasmic localization. Biochem J 2010;430:393–404.
65. Li X, Wang QJ, Pan N, Lee S, Zhao Y, Chait BT, et al. Phosphorylation-dependent 14-3-3 binding to LRRK2 is impaired by common mutations of familial Parkinson's disease. PLoS One 2011;6:e17153.
66. Dzamko N, Deak M, Hentati F, Reith AD, Prescott AR, Alessi DR, et al. Inhibition of LRRK2 kinase activity leads to dephosphorylation of Ser(910)/Ser(935), disruption of 14-3-3 binding and altered cytoplasmic localization. Biochem J 2010;430:405–413.